
Wasserstein GANs Work Because They Fail (to Approximate the Wasserstein Distance)

Jan Stanczuk¹ Christian Etmann¹ Lisa Maria Kreusser² Carola-Bibiane Schönlieb¹

Abstract

Wasserstein GANs (WGANs) are based on the idea of minimising the Wasserstein distance between a real and a generated distribution. We provide an in-depth mathematical analysis of differences between the theoretical setup and the reality of training WGANs. In this work, we gather both theoretical and empirical evidence that the WGAN loss is not a meaningful approximation of the Wasserstein distance. In addition, we argue that the Wasserstein distance is not a desirable loss function for deep generative models. We conclude that the success of WGANs can be attributed to the failure to approximate the Wasserstein distance.

1. Introduction

The Wasserstein GAN (WGAN), first introduced in (Arjovsky et al., 2017), is a framework for training Generative Adversarial Networks (GANs) by minimising the Wasserstein-1 distance (henceforth just called ‘the’ Wasserstein distance) between a real and a generated distribution. The use of the Wasserstein distance was motivated as a remedy for shortcomings of the Jensen-Shannon (JS) divergence, which is implicitly used in vanilla GANs (Goodfellow et al., 2014), but introduces some fundamental problems (Arjovsky & Bottou, 2017).

Over time, practical implementations of WGANs have continuously been improved. Improvements include WGANs with gradient penalty (WGAN-GP) (Gulrajani et al., 2017) or, for specific cases only, so-called StyleGANs (Karras et al., 2018). While the generative performance of WGANs has gained wide-spread interest, other works (Le et al., 2019b; Lunz et al., 2019) train WGANs specifically to

employ the trained discriminators (also called *critics*) to estimate Wasserstein distances.

In recent years, WGANs have become one of the most studied and successful deep generative models. Initially it was suggested that the success of WGANs can be attributed to the use of the Wasserstein distance. Many publications (Lei et al., 2019; Le et al., 2019a; Cho & Suh, 2019; Huang et al., 2019; Erdmann et al., 2018) (including some of our own prior work (Lunz et al., 2019) and educational materials (Weng, 2019) still propagate or even rely on the assumption that WGANs are capable of approximating the Wasserstein distance accurately and that an accurate approximation is desirable. However, the theoretical foundations of WGANs and the validity of the theoretical assumptions made in (Arjovsky et al., 2017) have received little attention so far. In the studies by Pinetz et al. (2019); Mallasto et al. (2019b), the authors examine certain failures of the approximation of the correct Wasserstein distance via WGAN-GP.

In our work, we take a critical look at the original motivation of WGANs. We explore both theoretical and practical shortcomings of WGANs, and conclude that real-world implementations of WGANs should not be thought of as Wasserstein distance minimisers. We show that certain theoretical assumptions on WGANs are not satisfied in practise and infer that aiming for an accurate approximation of the Wasserstein distance with a WGAN loss is counterproductive and leads to worse results. We argue that the original success of WGAN-GP is likely to be the result of the regularisation of the discriminator (via Lipschitz constraints) and can be regarded as a carefully-chosen hyperparameter configuration rather than as a new loss function.

We point out subtle differences between various possible notions of the ‘Wasserstein distance as a loss function’, including the ‘distributional’ Wasserstein distance and the ‘batch’ Wasserstein distance (for their definitions see Section 1.2). The batch Wasserstein distance is of interest in several works, see (Mallasto et al., 2019b;a; Fatras et al., 2020), where it has been examined as a potential loss function for WGAN-based generative models.

Sample complexity estimates (compare Section 5) show that estimating the true Wasserstein distance between dis-

¹Cambridge Image Analysis Group, Department of Applied Mathematics and Theoretical Physics, University of Cambridge, Cambridge, United Kingdom ²Department of Mathematical Sciences, University of Bath, Bath, United Kingdom. Correspondence to: Jan Stanczuk <js2164@cam.ac.uk>.

tributions via batches requires prohibitive batch sizes. We demonstrate that even with a favourable sample complexity (obtained via entropic regularisation), the generated samples of good batch Wasserstein estimators have a low fidelity.

For the case of Bernoulli measures, minimising batch Wasserstein distances leads to noticeably different minimisers than minimising the actual Wasserstein distance between data-generating distributions (Bellemare et al., 2017). Moreover, there is a non-vanishing bias in sample estimates of the gradient of Wasserstein distances which can have an influence on gradient descent based learning algorithms. We take this analysis further and show empirically that false or undesirable minima occur not only in the case of Bernoulli measures, but also while learning common synthetic and benchmark distributions.

We show that a perfect generator – one that outputs actual samples from the data set – yields a significantly higher batch Wasserstein distance on average than a distribution concentrated on the centroids of geometric k -medians clustering. We prove that in a certain sense, these centroids comprise the batch that has the optimal Wasserstein distance to the data set.

A variant of the batch Wasserstein distance has been suggested as a loss function for a generative model in (Fratras et al., 2020), but experiments are only provided for 2D Gaussian data. Based on our theory we predict that when applied to image data a model based on the batch Wasserstein distance results in blurry k -medians-like images which is also confirmed by our numerical experiments. We argue that the Wasserstein-1 distance is not a desirable loss function for deep generative models for image data due to the reliance on pixel-wise metrics, and we provide empirical evidence for this. We conclude that the success of WGANs can be attributed to the failure to approximate the Wasserstein distance.

While Mallasto et al. (2019b) suggests using the c -transform as a more accurate batch Wasserstein estimator, a worse generative performance has been observed. We demonstrate that the drop in performance is related to sample complexity and optimisation, but is also an issue of the Wasserstein distance itself due to the euclidean distance as the underlying metric.

This analysis raises a natural question: If models like WGAN-GP (which generate high-fidelity samples) do not use a meaningful approximation of the Wasserstein distance, why do they achieve said visual performance, often better than the vanilla GAN (Goodfellow et al., 2014)? The literature suggests two possible answers: Firstly, it has been proposed in (Kodali et al., 2017) and (Fedus et al., 2017) that regularising the Lipschitz constraint of the discriminator may improve stability of GAN training *regardless* of

the statistical distance used as a loss function. Secondly, in (Lucic et al., 2017), a large-scale experiment has shown that vanilla GANs can achieve similar performance to WGAN-GP if the right hyperparameters are chosen. Therefore, the original success of WGAN-GP might be due to a carefully-chosen hyperparameter configuration rather than because of the new loss function. Our observations agree with the points made in (Fedus et al., 2017) that GANs should not be understood as minimisers of some statistical distance. This suggests that the dynamics of the optimisation process based on alternating gradient updates need to be understood better and it is not sufficient to study the loss function or the optimal discriminator regime.

1.1. Contributions

The contributions of our work are as follows:

1. We provide a careful in-depth discussion on the modelling assumptions in (Arjovsky et al., 2017). We specify the different ways in which the training of WGANs can (and in practice, does) fail to approximate Wasserstein distance estimators and we demonstrate these claims by providing theoretical and empirical evidence.
2. We point out subtle differences between various possible notions of the ‘Wasserstein distance as a loss function’. We show that for the batch Wasserstein distance, sample complexity issues fail to fully explain the failure (first noted by (Mallasto et al., 2019b)) of good batch Wasserstein estimators to generate high-fidelity samples.
3. In addition to known results in (Bellemare et al., 2017), we demonstrate that the batch Wasserstein-1 distance is not even a desirable loss function for GANs. For this, we derive a new connection between the Wasserstein distance and clustering (geometric k -medians clustering), which results in undesirable, low-fidelity samples, that nevertheless exhibit a low Wasserstein distance. We provide an experiment which shows that on the contrary, even a perfect generator (outputting actual data samples) yields a comparatively large Wasserstein distance.
4. We argue that the fundamental problems of the Wasserstein-1 distance stem from the underlying euclidean metric. We suggest that the failure to approximate the Wasserstein distance accurately enables the generation of high-fidelity samples. In fact, the regularisation of the discriminator (in WGANs motivated by a Lipschitz constraint on the discriminator) helps generate good-looking samples, even when non-Wasserstein GANs are used.

1.2. Notation

In this work, we use the following notation.

- *Empirical measures*: Given a probability distribution p , we denote the *empirical measure* of n samples by p_n , defined by $p_n := \frac{1}{n} \sum_{i=1}^n \delta_{x_i}$, where x_i for $i = 1, \dots, n$ are independent and identically distributed (i.i.d.) samples from p . Thus, p_n represents a mini-batch of n samples from p and we can consider p_n as a distribution. We write $x \sim p_n$ if x is distributed according to p_n . The expectation of a given function f satisfies $\mathbb{E}_{x \sim p_n}[f(x)] = \int f(x)p_n(x)dx = \frac{1}{n} \sum_{i=1}^n f(x_i)$.
- *Set of empirical measures*: Given a probability distribution p , we denote the set of all empirical measures of n samples drawn from p by \mathcal{P}_n . We write $p_n \sim \mathcal{P}_n$ if we draw an empirical measure p_n from the set \mathcal{P}_n .
- *Lipschitz continuity*: For a Lipschitz continuous function f , we denote its Lipschitz constant with respect to the euclidean norm (both in the domain and co-domain) by $\|f\|_L$.
- *Wasserstein distance*: The Wasserstein distance is defined as

$$W_1(p^*, p^\theta) := \inf_{\gamma \in \Gamma(p^*, p^\theta)} \mathbb{E}_{(x,y) \sim \gamma} [\|x - y\|], \quad (1.1)$$

where the infimum is taken over all joint distributions γ with marginals p^* and p^θ . The above is referred to as the *primal formulation* of Wasserstein distance. The Kantorovich-Rubenstein duality is given by

$$W_1(p^*, p^\theta) = \max_{\|f\|_L \leq 1} (\mathbb{E}_{x \sim p^*}[f(x)] - \mathbb{E}_{x \sim p^\theta}[f(x)]). \quad (1.2)$$

This is referred to as the *dual formulation*. The maximiser f^* is called *Kantorovich's potential* between p^* and p^θ and is determined (up to a constant) by p^* and p^θ .

- *Oracle estimator*: Let the empirical measures p_n^*, p_n^θ associated with the probability distributions p^*, p^θ be given. We define the oracle estimator as

$$W_1^*(p_n^*, p_n^\theta) = \mathbb{E}_{x \sim p_n^*}[f^*(x)] - \mathbb{E}_{x \sim p_n^\theta}[f^*(x)],$$

where

$$f^* \in \arg \max_{\|f\|_L \leq 1} (\mathbb{E}_{x \sim p^*}[f(x)] - \mathbb{E}_{x \sim p^\theta}[f(x)]) \quad (1.3)$$

is Kantorovich's potential.

- *Mini-batch estimator*: Given empirical measures p_n^*, p_n^θ , we define the mini-batch estimator as

$$\hat{W}_1(p_n^*, p_n^\theta) = \max_{\|f\|_L \leq 1} (\mathbb{E}_{x \sim p_n^*}[f(x)] - \mathbb{E}_{x \sim p_n^\theta}[f(x)]).$$

- *Batch Wasserstein and distributional Wasserstein distance*: Sometimes we wish to emphasise the difference between $W_1(p_n^*, p_n^\theta)$ and $W_1(p^*, p^\theta)$. In such cases we refer to the former as *batch Wasserstein distance* and to the latter as *distributional Wasserstein distance*.

1.3. Outline

This paper is structured as follows. In Section 2, we give an overview on the original theory motivating the introduction of WGANs. In Section 3, we discuss how the Wasserstein distance is approximated in WGANs and distinguish two notions of Wasserstein distance as a loss function in the literature: the *batch Wasserstein distance* between mini-batches and the *distributional Wasserstein distance*. We examine how well different WGANs approximate the loss function in Section 4. We conclude that WGANs fail to approximate the distributional Wasserstein distance and that a better approximation of the Wasserstein distance between minibatches leads to worse generative performance. In Section 5, we explore how sample complexity makes the efficient approximation of distributional Wasserstein distance impossible. We further investigate false minima of the batch Wasserstein distance and their connection to clustering. In section 6, we discuss fundamental issues of the Wasserstein distance as a loss function for image data stemming from the fact that it is based on the pixelwise L_2 distance. In section 7, we discuss possible explanations for the initially reported success of WGAN in light of the failure to approximate Wasserstein distance.

2. Original Motivations for Wasserstein GAN

2.1. Theoretical formulation of GANs

Generative adversarial networks (GANs) were introduced in (Goodfellow et al., 2014) as a new framework for generative models. A GAN consists of two neural networks: the generator $G_\theta : \mathcal{Z} \rightarrow \mathcal{X}$ and the discriminator $D_\alpha : \mathcal{X} \rightarrow \mathbb{R}$ which compete against each other. Here, \mathcal{Z} denotes the latent space, \mathcal{X} is the data space and θ, α denote the parameters of the respective networks. The space \mathcal{Z} is usually endowed with a multivariate Gaussian distribution p_z . For $z \in \mathcal{Z}$ with $z \sim p_z$, the outputs of the generator $G_\theta(z)$ form a distribution which we call the *generator distribution* and denote by p^θ . The generator learns to produce samples which resemble the data from a *target distribution* p^* , while the discriminator is trying to distinguish fake from real data (by assigning an estimated probability that $D_\alpha(x)$ is 'real' rather than generated data). In the context of WGANs, the

discriminator is often called ‘critic’. Hence, we train D_α to maximize the probability of assigning the correct label to both training examples and samples from G_θ , while we train G_θ to minimise the discrepancy between the generated samples and data. Formally, given a value function $V(G_\theta, D_\alpha)$ the optimisation objective is of the form

$$\min_{\theta} \max_{\alpha} V(G_\theta, D_\alpha).$$

2.2. Optimal discriminator dynamics

A common approach to analysing the training of GANs is the so-called *optimal discriminator dynamics*. In the optimal discriminator dynamics approach, we define $F(G_\theta) := \max_{\alpha} V(G_\theta, D_\alpha)$ and analyse GANs as a minimisation problem (rather than a mini-max problem):

$$\min_{\theta} \max_{\alpha} V(G_\theta, D_\alpha) = \min_{\theta} F(G_\theta).$$

This approach to modelling GAN dynamics relies on what we call the *optimal discriminator assumption* (ODA), i.e. that after each update of the generator, we assume that the best possible discriminator was picked. This is not the case in practice, as we will discuss in later sections.

If we choose the right value function, we can interpret GAN training as a minimisation of a statistical divergence between a target and a generated distribution under the ODA. For example in (Goodfellow et al., 2014), it has been shown that vanilla GAN’s value function

$$\begin{aligned} V(G_\theta, D_\alpha) \\ = \mathbb{E}_{x \sim p^*} [\log D_\alpha(x)] + \mathbb{E}_{z \sim p_z} [\log(1 - D_\alpha(G_\theta(z)))] \end{aligned}$$

induces the minimisation of the Jensen-Shannon divergence

$$JS(p^*, p^\theta) = \frac{1}{2} \left(KL(p^* || \frac{p^* + p^\theta}{2}) + KL(p^\theta || \frac{p^* + p^\theta}{2}) \right)$$

between the real distribution p^* and the generator distribution p^θ where KL denotes the Kullback-Leibler divergence.

2.3. Choosing the right divergence

A rigorous mathematical analysis of the vanilla GAN’s optimal discriminator dynamics has been performed in (Arjovsky & Bottou, 2017). The authors prove that for the vanilla GAN’s value function, an accurate approximation of the optimal discriminator leads to vanishing gradients passed to the generator (i.e. $\nabla_{\theta} V(G_\theta, D_\alpha) \rightarrow 0$ as D_α approaches the optimal discriminator D^*). This problem can be traced back to the fact that the JS divergence is maximised whenever two distributions have disjoint supports. To address this issue, the authors in (Arjovsky et al., 2017) suggest to replace the JS divergence by the Wasserstein distance W_1 which decreases smoothly as the supports of the

distributions converge to each other. In order to apply the Wasserstein distance to GAN training, the authors use the Kantorovich-Rubenstein duality (1.2) and redefine the GAN objective function as

$$V(G_\theta, D_\alpha) = \mathbb{E}_{x \sim p^*} [D_\alpha(x)] - \mathbb{E}_{z \sim p_z} [D_\alpha(G_\theta(z))]. \quad (2.1)$$

The mini-max objective can be rewritten as

$$\min_{\theta} \max_{\|D_\alpha\|_L \leq 1} V(G_\theta, D_\alpha) = \min_{\theta} W_1(p^*, p^\theta), \quad (2.2)$$

which shows that the 1-Lipschitz functions act as the class of possible discriminators.

3. Estimation of W_1 in WGANs

3.1. WGAN-GP Algorithm

The exact computation of

$$W_1(p^*, p^\theta) = \max_{\|f\|_L \leq 1} (\mathbb{E}_{x \sim p^*} [f(x)] - \mathbb{E}_{x \sim p^\theta} [f(x)]) \quad (3.1)$$

is in practice impossible for two reasons. Firstly, it is computationally impossible to optimise over the set of all 1-Lipschitz functions accurately. Secondly, we do not have access to the full measures p^* and p^θ , but only to finite samples from each of them. Therefore, the Wasserstein distance has to be approximated via some tractable loss function in WGANs. There are many suggestions for loss functions in the literature (e.g. (Arjovsky et al., 2017; Gulrajani et al., 2017; Miyato et al., 2018)). We focus on the most prominent approximation scheme, introduced in (Gulrajani et al., 2017). The function f in the duality formula (3.1) is replaced by a neural network D_α , which is then trained to maximise (3.1). Moreover the network is (at least approximately) constrained to be a 1-Lipschitz function. For this reason a regularisation term called *gradient penalty* is incorporated in the loss function. More precisely, let p_n^* and p_n^θ denote the empirical measures associated with measures p^* and p^θ for the n samples $(x_i)_{i=1}^n$ and $(\tilde{x}_i)_{i=1}^n$, respectively. Define

$$\mathcal{V}(D_\alpha, p_n^*, p_n^\theta) := \mathbb{E}_{x \sim p_n^*} [D_\alpha(x)] - \mathbb{E}_{x \sim p_n^\theta} [D_\alpha(x)], \quad (3.2)$$

$$\mathcal{R}(D_\alpha, p_n^*, p_n^\theta) := \mathbb{E}_{x \sim \tau} [(\|\nabla_x D_\alpha(x)\| - 1)^2], \quad (3.3)$$

where $\tau := \tau(p_n^*, p_n^\theta)$ is defined as the uniform distribution on the lines connecting x_i with \tilde{x}_i for $i = 1, \dots, m$. Note that (3.2) can be regarded as an approximation of (2.1), while (3.3) enforces the gradient penalty.

Then one can optimise an approximation of the mini-max objective in (2.2) in an iterative fashion. First sample batches

p_n^*, p_n^θ and make a gradient ascent step with respect to the discriminator loss function $\mathcal{L}_D(\alpha) := \mathcal{V}(D_\alpha, p_n^*, p_n^\theta) - \lambda \mathcal{R}(D_\alpha, p_n^*, p_n^\theta)$. Repeat this process N_D times (to approximate $D_{\alpha^*} = \arg \max_{\|D_\alpha\|_L \leq 1} \mathcal{V}(G_\theta, D_\alpha)$). Then sample new batches p_n^*, p_n^θ and make a gradient descent step with respect to the generator loss $\mathcal{L}_G(\theta) := \mathcal{V}(D_\alpha, p_n^*, p_n^\theta)$. Repeat the whole procedure N_G times. The WGAN-GP is described in pseudo-code in the Algorithm 1.

Remark 1. In (3.2) we use a different notation for the value function \mathcal{V} instead of V in (2.1). First notice that $V(G_\theta, D_\alpha)$ in (2.1) depends on G_θ only through p^θ and hence we may regard V as a function of D_α and p^θ . Sometimes we want to refer explicitly to the value function evaluated using randomly sampled mini-batches p_n^* and p_n^θ . In this case we shall write $\mathcal{V}(D_\alpha, p_n^*, p_n^\theta)$ as in (3.2).

Algorithm 1: WGAN-GP

Input: N_G - number of generator updates, N_D - number of discriminator updates per one generator update, λ - gradient penalty regularisation parameter

```

for  $N_G$  iterations do
  for  $N_D$  iterations do
    Sample a batch  $p_n^*$  from  $p^*$ 
    Sample a batch  $p_n^\theta$  from  $p^\theta$ 
    Ascent  $\alpha$  wrt.
       $\mathcal{L}_D(\alpha) := \mathcal{V}(D_\alpha, p_n^*, p_n^\theta) - \lambda \mathcal{R}(D_\alpha, p_n^*, p_n^\theta)$ 
    end
    Sample a batch  $p_n^*$  from  $p^*$ 
    Sample a batch  $p_n^\theta$  from  $p^\theta$ 
    Descent  $\theta$  wrt.  $\mathcal{L}_G(\theta) := \mathcal{V}(D_\alpha, p_n^*, p_n^\theta)$ 
  end
end
    
```

Remark 2. In Algorithm 1 we could have removed the second sampling from p_n^* and descent wrt. $-\mathbb{E}_{x \sim p_n^\theta} [D_\alpha(x)]$ instead of $\mathcal{V}(D_\alpha, p_n^*, p_n^\theta)$. This would result in the same minimiser θ^* , but in such case $\mathcal{L}_G(\theta)$ would not approximate W_1 .

3.2. c -transform WGAN

An approximation scheme based on c -transform has been proposed in (Mallasto et al., 2019b) which gives a more accurate approximation of W_1 between mini-batches than WGAN-GP. The main idea of their approach is to replace the Kantorovich-Rubinstein duality with the following so-called *weak duality* formula:

Theorem 3.2.1 (Weak Duality, (Mallasto et al., 2019b)). For probability distributions p^*, p^θ , we have

$$W_1(p^*, p^\theta) = \sup_{f \in \mathcal{C}_b} \left(\mathbb{E}_{x \sim p^*} [f(x)] + \mathbb{E}_{x \sim p^\theta} [f^c(x)] \right),$$

where the supremum is taken over the space \mathcal{C}_b of all continuous bounded functions such that $f \in \mathcal{C}_b$ satisfies $f : \mathcal{X} \rightarrow \mathbb{R}$ and $f^c(x) := \sup_y \{f(y) - \|x - y\|\}$ is its c -transform of f .

Note that the c -transform of a 1-Lipschitz function f is given by $f^c = -f$. Hence, f^c is easy to compute for 1-Lipschitz functions. However, note that the optimisation is over the space of \mathcal{C}_b .

In the c -transform WGAN, the authors use the weak duality (Theorem 3.2.1) instead of Kantorovich-Rubinstein duality. This allows for the optimisation of the discriminator to be unconstrained, but introduces an approximate c -transform in the objective which reads

$$V(G_\theta, D_\alpha) = \mathbb{E}_{x \sim p^*} [f(x)] + \mathbb{E}_{x \sim p^\theta} [f^c(x)]$$

The mini-max objective can be rewritten as

$$\min_{\theta} \max_{\alpha} V(G_\theta, D_\alpha) = \min_{\theta} W_1(p^*, p^\theta).$$

Similarly to the WGAN-GP in Section 3, we consider the loss approximation

$$\mathcal{V}(D_\alpha, p_n^*, p_n^\theta) := \mathbb{E}_{x \sim p_n^*} [D_\alpha(x)] + \mathbb{E}_{x \sim p_n^\theta} [\hat{D}_\alpha^c(x)], \quad (3.4)$$

where \hat{D}_α^c is an approximation to c -transform of D_α given as $\hat{D}_\alpha^c(x) := \min_{y \in \text{supp}(p_n^\theta)} \|x - y\| - D_\alpha(y)$.

The algorithm for the c -transform WGAN is as in Algorithm 1, but with $\mathcal{L}_D(\alpha) = \mathcal{L}_G(\theta) = \mathcal{V}(D_\alpha, p_n^*, p_n^\theta)$ defined in (3.4)

3.3. The oracle estimator

The main idea behind the WGAN-GP algorithm is that D_α , optimised in the inner loop, approximates Kantorovich's potential between p^* and p^θ in (1.3). As a result the loss function of the generator approximates the *oracle estimator* of the Wasserstein distance

$$W_1^*(p_n^*, p_n^\theta) = \mathbb{E}_{x \sim p_n^*} [f^*(x)] - \mathbb{E}_{x \sim p_n^\theta} [f^*(x)],$$

where

$$f^* \in \arg \max_{\|f\|_L \leq 1} \left(\mathbb{E}_{x \sim p^*} [f(x)] - \mathbb{E}_{x \sim p^\theta} [f(x)] \right).$$

From the above discussion, we can conclude that there are two sources of error in the approximation of the Wasserstein distance:

1. Not learning the optimal discriminator exactly.
2. Estimation of the expectations based on finite samples.

We discuss the impact of each source of error in the following sections. Moreover, we notice that even if we approximate the Wasserstein distance perfectly we still need to perform a non-convex optimisation via a stochastic gradient descent based learning algorithm on $W_1(p^*, p^\theta)$ in order to successfully train a GAN.

3.4. The batch estimator

Recently, some researchers have examined how well the loss function of WGAN approximates the distance between random mini-batches (Mallasto et al., 2019b). More precisely, instead of approximating the oracle estimator they suggest that the loss function of WGAN should approximate the *batch estimator*

$$\hat{W}_1(p_n^*, p_n^\theta) = \max_{\|f\|_L \leq 1} (\mathbb{E}_{x \sim p_n^*}[f(x)] - \mathbb{E}_{x \sim p_n^\theta}[f(x)]).$$

Here we have following sources of error:

1. Not learning the optimal discriminator exactly.
2. Fitting the discriminator to p_n^* and p_n^θ instead of p^* and p^θ (sample complexity).

Using Theorem 3.2.1, the batch estimator can be written as

$$\hat{W}_1(p_n^*, p_n^\theta) = \sup_{f \in \mathcal{C}_b} (\mathbb{E}_{x \sim p_n^*}[f(x)] + \mathbb{E}_{x \sim p_n^\theta}[f^c(x)]).$$

4. Approximation of the optimal discriminator

In the following, we discuss how accurately the optimal discriminator D_α is approximated in the different methods for the estimation of the Wasserstein distance. In other words, we investigate whether the loss function of WGAN-GP \mathcal{L}_G satisfies the approximations $\mathcal{L}_G(\theta) \approx W_1^*(p^*, p^\theta)$ and $\mathcal{L}_G(\theta) \approx \hat{W}_1(p^*, p^\theta)$. This question has been explored in two recent works by Mallasto et al. (2019b) and Pinetz et al. (2019), but our experiments differ significantly. The subtle, but crucial differences are explained in detail in the Appendix B.

We show the following relations which are summarised in Figure 1:

- The loss function \mathcal{L}_G fails to approximate the oracle estimator $W_1^*(p^*, p^\theta)$ because the inner loop of Algorithm 1 fails to capture the optimal discriminator (Section 4.1).
- The loss function \mathcal{L}_G can approximate the batch estimator $\hat{W}_1(p^*, p^\theta)$ when trained using the c -transform, but $\hat{W}_1(p^*, p^\theta)$ is not a good approximation of the distribution level Wasserstein distance $W_1(p^*, p^\theta)$ (Section 4.2).

- The batch estimator $\hat{W}_1(p^*, p^\theta)$ of the Wasserstein distance $W_1(p^*, p^\theta)$ is not a desirable loss function for a generative model (Section 5).
- The close connection of the Wasserstein distance to the pixelwise L_2 norm causes fundamental issues when applying the Wasserstein distance to image data (Section 6).

This is unrealistic.
(Section 4.1)

$$\mathcal{L}_G(\theta) \approx W_1^*(p^*, p^\theta) \approx W_1(p^*, p^\theta)$$

$$\mathcal{L}_G(\theta) \approx \hat{W}_1(p^*, p^\theta) \approx W_1(p^*, p^\theta)$$

This is possible with c -transform.
(Section 4.2) This is impossible due to sample complexity.
(Section 5)

Figure 1: Overview of the desired approximations of \mathcal{L}_G .

4.1. Approximation of the oracle estimator

First, we examine whether

$$\mathcal{L}_G(\theta) \approx W_1^*(p^*, p^\theta) \quad (4.1)$$

is a valid approximation. This is the case if and only if the inner loop of the WGAN-GP algorithm 1, also called the *discriminator loop*, computes a good approximation D_α of Kantorovich’s potential f^* in (1.3).

4.1.1. APPROXIMATION FOR FIXED, FINITELY SUPPORTED DISTRIBUTIONS

To examine whether (4.1) is satisfied in practice, we design the following experiment, summarised in Algorithm 2. We pick two large finitely supported distributions p^* and p^θ , each consisting of 10K images from CIFAR-10 (Krizhevsky, 2009). Then we sample mini-batches (of size $n = 64$) from p^* , p^θ and maximise $\mathcal{L}_D(\alpha)$. This is exactly the same procedure as in the WGAN-GP training in Algorithm 1 except that both measures are static (as if the generator in Algorithm 1 was frozen). We consider $N = 300K$ updates for D_α . At the end, we check if the approximation

$$\begin{aligned} W_1^D(p^*, p^\theta) &= \mathcal{V}(D_\alpha, p^*, p^\theta) \\ &= \mathbb{E}_{x \sim p^*}[D_\alpha(x)] - \mathbb{E}_{x \sim p^\theta}[D_\alpha(x)] \end{aligned}$$

is close to $W_1(p^*, p^\theta)$. Note that we return $\mathcal{V}(D_\alpha, p^*, p^\theta)$ and not $\mathcal{V}(D_\alpha, p^*, p^\theta) - \lambda \mathcal{R}(D_\alpha, p^*, p^\theta)$ for $W_1^D(p^*, p^\theta)$ in case the Lipschitz penalty is not well satisfied.

Since the distributions are finitely supported, $W_1(p^*, p^\theta)$ can be obtained by solving a linear program (LP) as in (Flamary et al., 2021). Note that superficially similar experiment to Algorithm 2 have been performed in (Pinetz et al., 2019)

Algorithm 2: Quality of oracle estimation for static distributions.

for N iterations **do**

 Sample a batch p_n^* from p^*
 Sample a batch p_n^θ from p^θ
 Ascent step on D_α wrt.
 $\mathcal{V}(D_\alpha, p_n^*, p_n^\theta) - \lambda \mathcal{R}(D_\alpha, p_n^*, p_n^\theta)$

end

$W_1^D(p^*, p^\theta) \leftarrow \mathbb{E}_{x \sim p^*}[D_\alpha(x)] - \mathbb{E}_{x \sim p^\theta}[D_\alpha(x)]$

$W_1(p^*, p^\theta) \leftarrow$ Solution of LP for p^*, p^θ

Compare $W_1^D(p^*, p^\theta)$ and $W_1(p^*, p^\theta)$

and (Mallasto et al., 2019b). Subtle, but crucial differences in the design of the experiment are discussed in Appendix B.

Notice that if $D_\alpha \approx f^*$ then $W_1^D(p^*, p^\theta) \approx W_1(p^*, p^\theta)$. Therefore we can assess the quality of the approximation of the optimal discriminator D_α in WGAN-GP by examining how much $W_1^D(p^*, p^\theta)$ differs from $W_1(p^*, p^\theta)$.

Remark 3. As pointed out in (Arjovsky et al., 2017) if we optimise over the set of K -Lipschitz functions instead of the set of 1-Lipschitz functions, then the estimate of Wasserstein distance scales by the same factor, i.e.

$$\max_{\|f\|_L \leq K} (\mathbb{E}_{x \sim p^*}[f(x)] - \mathbb{E}_{x \sim p^\theta}[f(x)]) = KW_1(p^*, p^\theta).$$

Since the 1-Lipschitz continuity of D_α is only approximately enforced in WGAN-GP, a normalisation by the Lipschitz constant of D_α should be considered. We define the lower bound of $\|D_\alpha\|_L$ by $\hat{L}(D_\alpha) := \max_{x \in \text{supp}(\tau)} \|\nabla D_\alpha(x)\|$ and consider the *normalised Wasserstein estimate* as $W_1^D(p^*, p^\theta) / \hat{L}(D_\alpha)$. This normalised quantity should be compared with $W_1(p^*, p^\theta)$.

In the experiments in Figures 2 and 3, we use Algorithm 2. We find that normalised Wasserstein estimate is very far from the actual $W_1(p^*, p^\theta)$. Since $W_1(p^*, p^\theta) = 41.21$, the normalised Wasserstein estimate $W_1^D(p^*, p^\theta) / \hat{L}(D_\alpha)$ is one order of magnitude smaller than $W_1(p^*, p^\theta)$. In the experiments in Figure 2 we explored a range of hyperparameters (λ , batch size, learning rate, network architecture). For the experiments visualized in Figure 3 we use the hyperparameters recommended in the original WGAN-GP paper (Gulrajani et al., 2017) except for the parameter λ which we allowed to vary. This allows us to explore how the value of λ influences the Lipschitz constraint and how it impacts the quality of Wasserstein estimation.

We emphasise that the task of estimating $W_1(p^*, p^\theta)$ in Algorithm 2 is easier than estimating $W_1(p^*, p^\theta)$ during WGAN training. Distributions p^* and p^θ are static, while p^θ changes after each N_D updates to the discriminator D_α in Algorithm 1. During WGAN training typically $N_D \leq 10$,

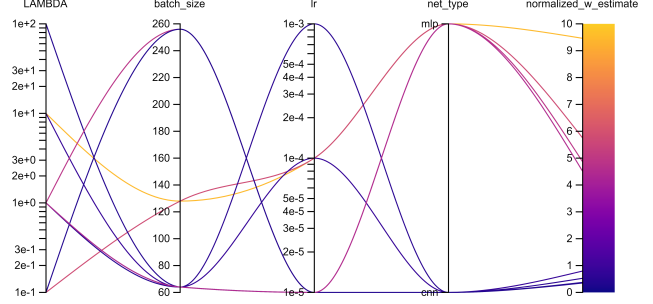


Figure 2: Estimated Wasserstein distance for different hyper-parameter configurations. The correct value is $W_1(p^*, p^\theta) = 41.21$. (Hyperparameter optimisation and plot done using (Biewald, 2020)).

while we allowed D_α to be trained for $N = 300K$ iterations on the same pair of distributions. The fact that even this simpler task cannot be accomplished implies that the approximation of the Wasserstein distance during WGAN training is unrealistic with WGAN-GP algorithm 1.

We point out that we are conservative in our approach to normalize the Wasserstein estimate since

$$\frac{W_1^D(p^*, p^\theta)}{\|D_\alpha\|_L} \leq \frac{W_1^D(p^*, p^\theta)}{\hat{L}(D_\alpha)} \ll W_1(p^*, p^\theta),$$

where the first inequality follows from $\hat{L}(D_\alpha) \leq \|D_\alpha\|_L$, and the second inequality is supported by Figure 3.

We conclude that $\mathcal{L}_G(\theta) \approx W^*(p^*, p^\theta)$ is not achieved in WGAN-GP, so the loss of WGAN-GP is not an accurate approximation of Wasserstein distance.

4.1.2. APPROXIMATION DURING TRAINING IN LOW DIMENSIONS

In this section, we investigate whether $\mathcal{L}_G(\theta) \approx W^*(p^*, p^\theta)$ can be achieved for the special case of low dimensions where sample complexity issues (discussed in detail in Section 5) can be neglected. In low dimensions, we can approximate $W_1(p^*, p^\theta)$ accurately by $W_1(p_n^*, p_n^\theta)$ for a sufficiently large number of samples n (we used $n = 1000$ for this experiment). Since p_n^*, p_n^θ are finite measures, we can determine $W_1(p_n^*, p_n^\theta)$ by solving the linear program and we can check how close $\mathcal{L}_G(\theta)$ is to $W_1(p^*, p^\theta)$ during a WGAN training.

We conduct an experiment where we fit the WGAN-GP in Algorithm 1 to an 8-mode Gaussian mixture and track $\mathcal{L}_G(\theta)$, $W_1(p^*, p^\theta)$ at each iteration. As discussed in Remark 3 we normalize the loss by $\hat{L}(D_\alpha)$ as the Lipschitz constraints in WGAN-GP are only approximated. In Figure 4, we show 250 samples from p^* and p^θ . The associated Wasserstein distance $W_1(p^*, p^\theta)$ and the normalised Wasser-

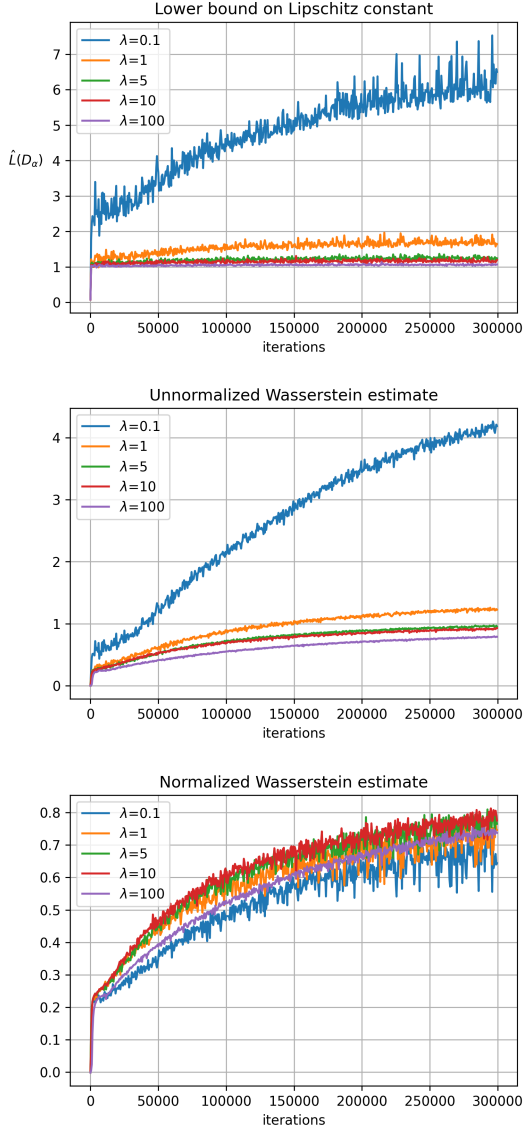


Figure 3: Estimated Wasserstein distance for different values of λ ($\lambda = 10$ is recommended in (Gulrajani et al., 2017)). All WGAN-GP approximations are very far from the correct value of $W_1(p^*, p^\theta) = 41.21$.

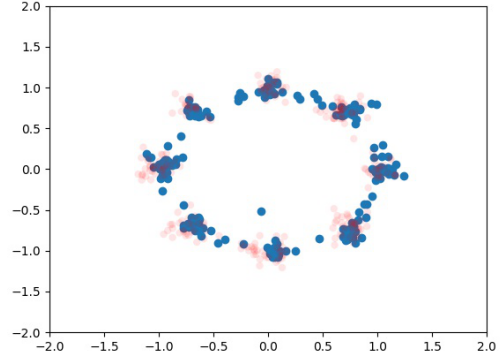


Figure 4: Blue dots are samples from p^θ and red dots are samples from p^* .

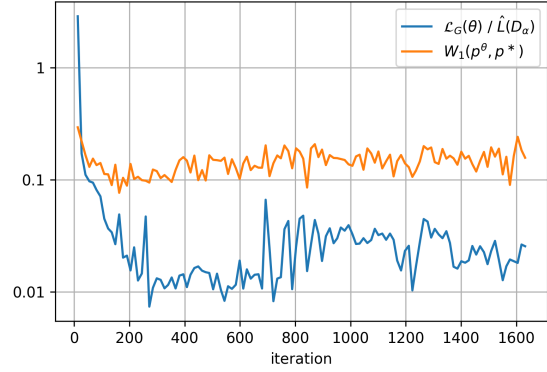


Figure 5: Normalized loss and true Wasserstein distance in log scale. At the end of the training the Wasserstein distance is 6.92 times higher than the normalized loss.

stein estimate $\mathcal{L}_G(\theta) / \hat{L}(D_\alpha)$ obtained with Algorithm 1 are shown in Figure 5. We observe that the normalised loss is an order of magnitude smaller the $W_1(p^*, p^\theta)$ as in the Experiments in Section 4.1.1. Notice that any sensible positive loss function will be close to zero. Again we conclude that even in a simple two dimensional case $\mathcal{L}_G(\theta) \approx W_1(p^*, p^\theta)$ is not achieved.

4.2. Approximation of the batch estimator

In this section we examine whether

$$\mathcal{L}_G(\theta) \approx \hat{W}_1(p^*, p^\theta).$$

We consider two algorithms: WGAN-GP (Gulrajani et al., 2017) and c-transform WGAN (Mallasto et al., 2019b). We reproduce the experiment of (Mallasto et al., 2019b) in a higher resolution setup and we use an improved architecture. For experiments in this section, we use the architecture based on StyleGAN (Karras et al., 2018) and CelebA data

set (Liu et al., 2015).

As in (Mallasto et al., 2019b), we train WGAN according Algorithm 1. At the end of each iteration of the generator loop we solve the linear program to evaluate the true Wasserstein distance $W_1(p_n^*, p_n^\theta)$ between the generated batch p_n^θ and the batch of the real data p_n^* . Then we compare the result with $\mathcal{L}_G(\theta)$. For c -transform WGAN $\mathcal{L}_G(\theta)$ is computed using the equation 3.4.

A detailed description of the experiment is included as Algorithm 3.

Algorithm 3: Experiment 2: Mini-batch estimator during WGAN training

```

for  $N_G$  iterations do
  for  $N_D$  iterations do
    Sample a batch  $p_n^*$  from  $p^*$ 
    Sample a batch  $p_n^\theta$  from  $p^\theta$ 
    Ascent  $\alpha$  wrt.  $\mathcal{L}_D(\alpha)$ 
  end
  Sample a batch  $p_n^*$  from  $p^*$ 
  Sample a batch  $p_n^\theta$  from  $p^\theta$ 
   $W_1(p_n^*, p_n^\theta) \leftarrow$  Solution of LP for  $p_n^*, p_n^\theta$ 
  Compare  $W_1(p_n^*, p_n^\theta)$  with
     $\mathcal{L}_G(\theta) = \mathcal{V}(D_\alpha, p_n^*, p_n^\theta)$ 
  Descent  $\theta$  wrt.  $\mathcal{L}_G(\theta)$ 
end
    
```

As shown in Figure 6, the gradient penalty the gradient penatly method does not provided an accurate approximation of \hat{W}_1 . On the other hand, the c -transform method approximates \hat{W}_1 very accurately. Surprisingly, a good approximation of the batch Wasserstein distance does not correspond to a good generative performance. Figure 7 shows samples obtained from training with the c -transform and the gradient penalty as the approximation method. The faces generated by a WGAN using the c -transform approximation look very blurry, while the WGAN-GP results look realistic. In particular, the images obtained with WGAN using the c -transform do not capture the complexity of the data set as well as WGAN-GP, despite achieving a better approximation of the Wasserstein distance. Moreover the loss function of WGAN-GP $\mathcal{L}(G)$ doesn't decrease despite the samples getting better with more training. This is because the loss of WGAN-GP reflects how well the generator performs compared to the discriminator, not the Wasserstein distance.

So we are left with a puzzling question: *Why does a better approximation of the batch Wasserstein distance result in a worse generative performance?*

In next sections, we examine possible explanations based on sample complexity, biased gradients and connections of

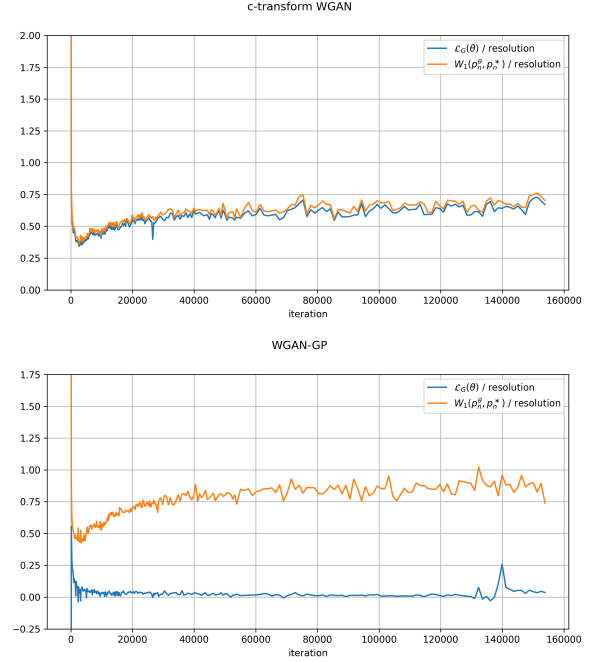


Figure 6: Plots show how accurately W_1 between training batches is approximated by a given method during WGAN training on the CelebA data set. Based on (Mallasto et al., 2019b).

W_1 to the L_2 -norm and clustering.

5. Finite sample approximation of W_1

In the following, we analyse problems arising from the fact that we use finite data and minibatch-based optimisation to estimate the Wasserstein distance between high dimensional distributions.

5.1. Sample complexity of Wasserstein distance estimators

Recall that the oracle estimator is defined as

$$W_1^*(p_n^*, p_n^\theta) = \mathbb{E}_{x \sim p_n^*} [f^*(x)] - \mathbb{E}_{x \sim p_n^\theta} [f^*(x)],$$

where $f^* \in \arg \max_{\|f\|_L \leq 1} (\mathbb{E}_{x \sim p^*} [f(x)] - \mathbb{E}_{x \sim p^\theta} [f(x)])$.

In the oracle estimator, the only effect of finite samples is the Monte Carlo approximation of the expectations which has a convergence rate of $O(\frac{1}{\sqrt{n}})$ when n samples are considered for p_n^*, p_n^θ . The oracle estimator assumes that we have access to an oracle which provides us with Kantorovich's potential f^* between p^* and p^θ . Therefore, the true sample complexity is moved to the oracle and the above convergence rate is misleading. An efficient oracle does not exist and in practice, one needs huge number of samples to be

able to accurately estimate f^* .

For the batch estimator

$$\hat{W}_1(p_n^*, p_n^\theta) = \max_{\|f\|_L \leq 1} (\mathbb{E}_{x \sim p_n^*}[f(x)] - \mathbb{E}_{x \sim p_n^\theta}[f(x)]),$$

we have $\hat{W}_1(p_n^*, p_n^\theta) = W_1(p_n^*, p_n^\theta)$ and the sample complexity is well known. As shown in (Weed & Bach, 2017), for d -dimensional data, the expected error of the estimation of the Wasserstein distance decreases as $O(n^{-1/d})$, i.e.

$$\mathbb{E}_{\substack{p_n^* \sim \mathcal{P}_n^* \\ p_n^\theta \sim \mathcal{P}_n^\theta}} [|W_1(p_n^*, p_n^\theta) - W_1(p^*, p^\theta)|] = O(n^{-1/d}),$$

where \mathcal{P}_n^* and \mathcal{P}_n^θ denote the sets of all empirical measures of n samples drawn from p^* and p^θ , respectively. This decay rate is very slow in high dimensions, and hence, even if the optimal discriminator between p_n^* and p_n^θ is learned perfectly, the loss function of WGAN is very far away from the actual Wasserstein distance.

In the following sections, we argue that sample complexity issues render the oracle estimator unrealistic and the mini-batch estimator useless.

5.2. Empirical study of sample complexity issues

In this empirical study, we illustrate that the sample size necessary for an accurate Wasserstein approximation is infeasible in the setting of high dimensional deep generative modelling. To this aim, we examine the difference between $W_1(p_n^*, \tilde{p}_n^*)$ and $W_1(p^*, p^*) = 0$ numerically where p^* is a standard Gaussian measure in d dimensions, and p_n^*, \tilde{p}_n^* are empirical measures of n samples drawn from p^* . Note that $W_1(p_n^*, \tilde{p}_n^*)$ decreases to 0 as $n \rightarrow \infty$ and the convergence is $O(n^{-1/d})$.

The sample Wasserstein distance concentrates very well around its expectation (Weed & Bach, 2017). Therefore, the behaviour of the random variable $W_1(p_n^*, \tilde{p}_n^*)$ can be understood by examining

$$\mathbb{E}_{p_n^* \sim \mathcal{P}_n^*, \tilde{p}_n^* \sim \mathcal{P}_n^*} [W_1(p_n^*, \tilde{p}_n^*)],$$

where \mathcal{P}_n^* denotes the set of all empirical measures of n samples drawn from p^* .

According to the *manifold hypothesis* (Narayanan & Mitter, 2010) the distribution p^* which we want to learn is concentrated around a lower dimensional manifold \mathcal{M} . According to results in (Weed & Bach, 2017) the dimension of \mathcal{M} , known as the *intrinsic dimension* of p^* , is relevant for the sample complexity of the Wasserstein distance and may be smaller than the dimension of the ambient Euclidean space. The dimension of the manifold modeled by a GAN is at most the dimension of its latent space \mathcal{Z} (Arjovsky & Bottou, 2017). Therefore, ideally we want to set the dimension

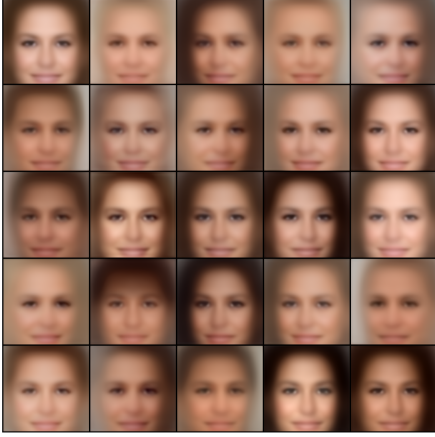


Figure 7: Samples resulting from the training with a given approximation method. c -transform on the top and gradient penalty on the bottom. Based on (Mallasto et al., 2019b).

of \mathcal{Z} to match the dimension of \mathcal{M} , although, when training GANs in practice, the dimension of \mathcal{Z} is often set to 100 or more (Radford et al., 2016; Karras et al., 2018).

Recent research on the intrinsic dimension suggests that benchmark data sets like CIFAR-10 and CelebA could have an intrinsic dimension of around 20 (Pope et al., 2021). To illustrate that the sample size necessary for an accurate Wasserstein approximation is infeasible for high-dimensional deep generative modelling, we examine the case of $d = 20$ for the Wasserstein distance between two random samples from the standard Gaussian distribution in Figure 8. In our experiments, we sample $N = 300$ pairs of batches p_n^*, \hat{p}_n^* for $n \in \{10, 25, 50, 75, 1000, 10000\}$ from p^* and calculate the corresponding Wasserstein distance $W_1(p_n^*, \hat{p}_n^*)$. Then we use a standard Monte Carlo estimator to approximate $\mathbb{E}_{p_n^* \sim \mathcal{P}_n^*, \hat{p}_n^* \sim \mathcal{P}_n^*}[W_1(p_n^*, \hat{p}_n^*)]$. Even for very large batches (up to 10,000) and for a simple Gaussian distribution, the estimation of the true Wasserstein distance ($=0$) is extremely bad.

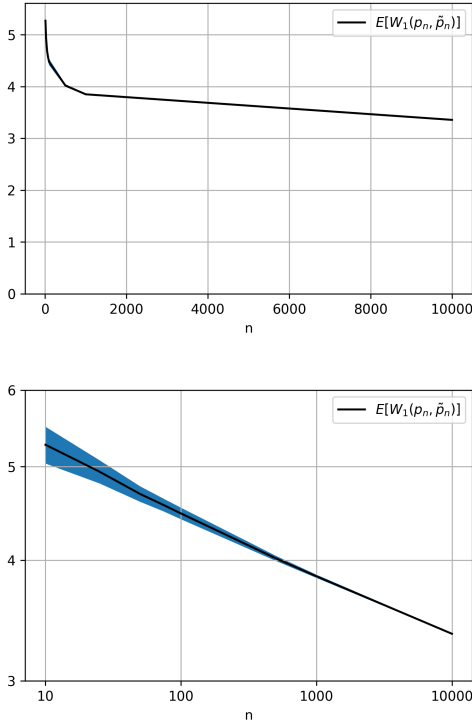


Figure 8: The figure shows the averaged (estimated using 100 repetitions of the experiment, blue bar shows standard deviation) W_1 between two random samples from standard Gaussian distribution in dimension 20 as a function of the sample size. Second plot is in log-log scale. The distance converges to zero extremely slowly rendering accurate Wasserstein estimation impossible.

Using the fact that in log-log space the relationship is linear,

we fit a least squares line and extrapolate for larger values of n in Figure 9. In this way we establish that in order to bring the approximation error to 0.1 one would need over 10^{20} samples, which is much larger than any conceivable data set. In order to bring the error down to 0.01 one would need over 10^{40} samples.

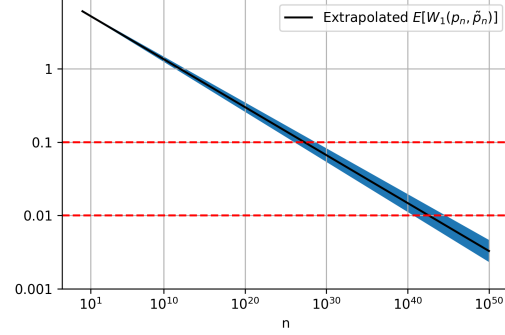


Figure 9: Extrapolation in log-log scale. Blue bar is the 95% confidence interval.

5.3. False minima of the batch Wasserstein distance

Given a target distribution p^* and generated distribution p^θ with parameter θ , the difference between the true Wasserstein distance $W_1(p^*, p^\theta)$ and its sample estimate $W_1(p_n^*, p_n^\theta)$ may cause the existence of ‘false’ global optima, i.e. $\min_\theta \mathbb{E}_{p_n^* \sim \mathcal{P}_n^*, p_n^\theta \sim \mathcal{P}_n^\theta}[W_1(p_n^*, p_n^\theta)]$ may be different from $\min_\theta W_1(p^*, p^\theta)$, where \mathcal{P}_n^* and \mathcal{P}_n^θ denote the sets of all empirical measures of n samples drawn from p^* and p^θ , respectively.

An example of this phenomenon has already been pointed out in (Bellemare et al., 2017). The authors demonstrate that false global minima may appear when one tries to learn a Bernoulli measure by minimising the batch Wasserstein distance. For the target Bernoulli measure p^* and the generated Bernoulli measure p^θ with parameter $\theta \in (0, 1)$, they show that the sample estimate of the Wasserstein gradient $\nabla_\theta W_1(p_n^*, p_n^\theta)$ is a biased estimator of $\nabla_\theta W_1(p^*, p^\theta)$. These estimation errors can strongly affect the training via stochastic gradient descent (SGD) or SGD-based algorithms like Adam. Their results are summarised in the following theorem:

Theorem 5.3.1. (Bellemare et al., 2017)

1. *Non-vanishing mini-max bias of the sample gradient.* For any $n \geq 1$ there exists a pair of Bernoulli distributions p^*, p^θ such that

$$|\mathbb{E}_{p_n^* \sim \mathcal{P}_n^*}[\nabla_\theta W_1(p_n^*, p_n^\theta)] - \nabla_\theta W_1(p^*, p^\theta)| \geq 2e^{-2}.$$

2. *Wrong minimum of the batch Wasserstein loss.* For

Bernoulli measures p^*, p^θ , the minimum of the expected sample loss

$$\bar{\theta} = \arg \min_{\theta} \mathbb{E}_{p_n \sim \mathcal{P}_n^*} [W_1(p_n^*, p^\theta)]$$

is in general different from the minimum of the true Wasserstein loss $\theta^* = \arg \min_{\theta} W_1(p^*, p^\theta)$.

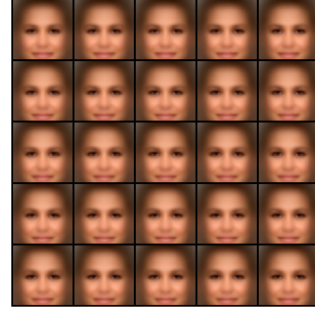
While Theorem 5.3.1 shows that minima of the distributional and the batch Wasserstein distance may not coincide, we investigate the existence of ‘false’ minima of the batch Wasserstein distance further in the context of WGAN training and show empirically that false minima can appear while learning synthetic (e.g. Gaussian) and benchmark distributions (e.g. CelebA (Liu et al., 2015)). For this, we consider certain fixed batches (a ‘real batch’ \tilde{p}_n^* , a ‘mean batch’ p^μ and a ‘geometric k -medians batch’ $p^{k\text{-gm}}$). We show empirically that in sufficiently high dimensions the expected Wasserstein distance between these batches and $p_n^* \sim \mathcal{P}_n^*$ is largest for $\mathbb{E}_{p_n^* \sim \mathcal{P}_n^*} [W_1(p_n^*, \tilde{p}_n^*)]$, even though p_n^*, \tilde{p}_n^* are both empirical measures with samples drawn from p^* and $W_1(p^*, p^*) = 0$. This is achieved by approximating the expectation with the standard Monte Carlo estimator using 100 sample batches from p^* . We conclude that a ‘mean batch’ or a ‘geometric k -medians batch’ provide false minima in the case of the CelebA data set.

The results of the above experiment are visualised in the Figure 10 for CelebA. We show that the expected batch Wasserstein distance between two samples from the target distribution $\mathbb{E}_{p_n^* \sim \mathcal{P}_n^*} [W_1(p_n^*, \tilde{p}_n^*)]$ is greater than the expected batch Wasserstein distance between a sample from the target distribution and a sample consisting of repeated means $\mathbb{E}_{p_n^* \sim \mathcal{P}_n^*} [W_1(p_n^*, p^\mu)]$ (or geometric k -medians). Therefore, a *perfect* generator producing samples from the target distribution p^* would have (on average) a greater loss than a generator which learned a Dirac distribution concentrated at the mean of p^* . Hence, the batch Wasserstein distance can push the generator towards false minima making it an undesirable loss function.

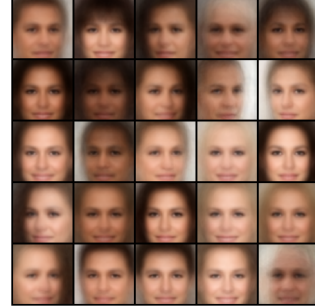
Next we compare $\mathbb{E}_{p_n^* \sim \mathcal{P}_n^*} [W_1(p_n^*, \tilde{p}_n^*)]$ and $\mathbb{E}_{p_n^* \sim \mathcal{P}_n^*} [W_1(p_n^*, p^\mu)]$ for the case where p^* is the standard Gaussian distribution and p^μ is a Dirac distribution concentrated at its mean, as a function of dimension d . As before, the expectation is approximated with the standard Monte Carlo estimator using 100 sample batches from p^* . The results are visualized on Figure 11. Again we observe that in sufficiently high dimension ($d > 15$) we have $\mathbb{E}_{p_n^* \sim \mathcal{P}_n^*} [W_1(p_n^*, p^\mu)] < \mathbb{E}_{p_n^* \sim \mathcal{P}_n^*} [W_1(p_n^*, \tilde{p}_n^*)]$. Therefore as in the case of the CelebA dataset, a generator producing samples from the target Gaussian distribution p^* has (on average) a greater batch Wasserstein loss than a generator which learned a Dirac distribution concentrated at the mean of p^* in high dimensions.



(a) $\mathbb{E}_{p_n^* \sim \mathcal{P}_n^*} [W_1(p_n^*, \tilde{p}_n^*)] = 50.67$



(b) $\mathbb{E}_{p_n^* \sim \mathcal{P}_n^*} [W_1(p_n^*, p^\mu)] = 47.91$



(c) $\mathbb{E}_{p_n^* \sim \mathcal{P}_n^*} [W_1(p_n^*, p^{k\text{-gm}})] = 39.44$

Figure 10: Three batches and their respective batchwise Wasserstein distance (for CelebA). We observe that a batch \tilde{p}_n of real faces (Fig. 10a) has higher batchwise W_1 -distance than undesirably simple generated batches: In particular, both a batch p^μ of the ‘average face’ (Fig. 10b), as well as a batch $p^{k\text{-gm}}$ of the k centroids of geometric k -medians clustering (Fig. 10c) over the data set (for $k = n$) yield far lower batchwise W_1 -distance than real data.

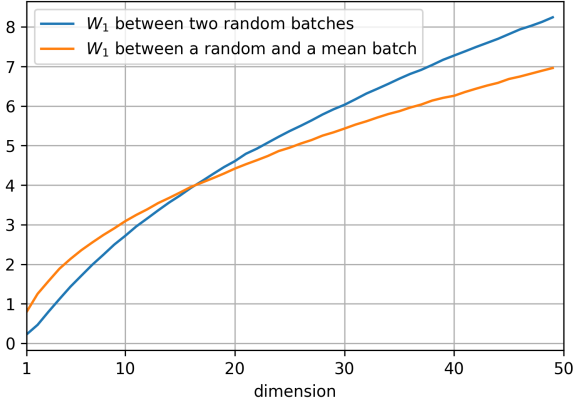


Figure 11: In sufficiently high dimension, a distribution concentrated on the mean has (on average) a smaller batch Wasserstein distance from a random sample of p^* than another random sample of p^* . Here, we can see this in the case of the Gaussian measure.

5.4. Connection to clustering

As we pointed out in Section 4.2, training a WGAN using the c -transform results in a better approximation of the batch Wasserstein distance, but achieves much worse generative performance than WGAN-GP. Moreover, as one can observe in Figure 12, the output of the c -transform WGAN looks very similar to geometric k -medians clustering.

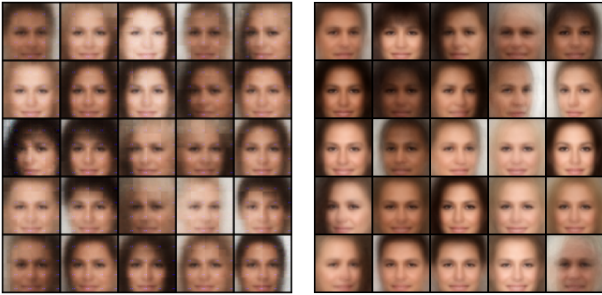


Figure 12: On the left: Output of WGAN trained with c -transform (Mallasto et al., 2019b). On the right: centroids produced by geometric k -medians clustering.

As discussed in Section 5.2, clustering may provide samples of low batch Wasserstein distance with low visual fidelity. (Canas & Rosasco, 2012) show a connection between k -medians clustering and the Wasserstein-2 distance. Here, we extend these results to the Wasserstein-1 distance W_1 , which is the basis for Wasserstein GANs. Our result establishes a connection between W_1 and geometric k -medians clustering.

The well-known k -means clustering determines cluster cen-

troids so that the sum of the *squared* euclidean distances of the cluster elements to their respective centroid is minimal. Suppose we are given a finite set $\mathcal{X} \subseteq \mathbb{R}^d$. Given an arbitrary set $S = \{m_i, i = 1, \dots, k\} \subseteq \mathbb{R}^d$, let $S_i = \{x \in \mathcal{X} : m_i = \arg \min_{m \in S} \|m - x\|_2\}$, i.e. S_i consists of points in \mathcal{X} for which the closest point in S is m_i . K-means is the solution to the optimisation problem

$$\arg \min_{S \subseteq \mathbb{R}^d: |S|=k} \sum_{i=1}^k \sum_{x \in S_i} \|m_i - x\|_2^2.$$

If we replace the squared euclidean distance by the (un-squared) euclidean distances, we obtain geometric k -medians clustering, given by

$$\arg \min_{S \subseteq \mathbb{R}^d: |S|=k} \sum_{i=1}^k \sum_{x \in S_i} \|m_i - x\|_2.$$

Note that for an arbitrary finite subset S of an euclidean space

$$\arg \min_m \sum_{x \in S} \|m - x\|_2$$

is called the *geometric median* of S . Unlike in the case of squared distances (where the arithmetic mean provides the respective minimiser), iterative algorithms have to be used for computing the geometric median of a set. In this work, we use Weiszfeld’s algorithm (Weiszfeld, 1937) to calculate the geometric median.

As for k -means clustering, finding the true, globally optimal clustering is infeasible in practice due to the NP-hardness of the problem. We employ the standard Lloyd’s algorithm (Lloyd, 1982) for clustering, which is a popular choice for k -means clustering. In contrast to k -means clustering (where centroids are computed via the arithmetic mean), we use Weiszfeld’s algorithm to compute the centroids, which lie in the geometric medians of the individual clusters. We initialise our clustering method with the k -means clustering method in `scikit-learn` (Pedregosa et al., 2011), as we noticed that the geometric medians lie quite close to the arithmetic means in practice. We used 100 different random initialisations for the k -means clustering to find the best loss for the geometric k -medians clustering.

Let $p^{k\text{-gm}}$ be an empirical measure formed by geometric k -medians centroids. Similarly to the results for the Wasserstein-2 distance (Canas & Rosasco, 2012), we show that in fact

$$p^{k\text{-gm}} = \arg \min_{|\text{supp}(p)|=k} W_1(p, p^*)$$

in Theorem A.1.3. This means that the distribution concentrated at the centroids of geometric k -medians has the

smallest W_1 distance from the target distribution p^* among all distributions supported on k points.

This result could shed some light on why geometric k -medians clustering creates undesirable minima for the batch Wasserstein distance. Training data comes in mini-batches and if we set the mini-batch size as k , then the batch consisting of geometric k -medians centroids is the mini-batch with the smallest possible loss.

There are still some differences between this analysis and the actual WGAN training which is based on the batch Wasserstein distance. We use a sample p_k^* from the target measure, rather than the full target measure p^* . Hence, when using batch estimator as loss, we actually minimise

$$\mathbb{E}_{\substack{p_k^* \sim \mathcal{P}_k^* \\ p_k^\theta \sim P_k^\theta}} [W_1(p_k^*, p_k^\theta)]$$

wrt. θ . We leave the problem of formally extending Theorem A.1.3 as a possible objective for further study. We notice that in Section 5.3 we have already seen empirically (in the case of CelebA) that $\mathbb{E}[W_1(p_k^{\text{gmm}}, p_k^*)] < \mathbb{E}[W_1(p_k^*, \tilde{p}_k^*)]$, where p_k^*, \tilde{p}_k^* are two empirical measures, each formed by k i.i.d. samples from p^* .

6. Fundamental issues of the Wasserstein distance with image data

In the previous sections, we have argued several ways, in which WGANs may fail to learn the Wasserstein distance.

- In Section 4.1, we saw that WGANs used in practice distinctly fail to approximate the true oracle discriminator f^* , i.e. they fail to minimise the distributional Wasserstein distance.
- In Section 4.2, we saw that WGANs with gradient penalties distinctly fail to approximate the batch Wasserstein distance.
- As elaborated in Sections 5.1 and 5.2, (batch) Wasserstein estimators require larger data sets than feasible in practice in order to accurately approximate the distributional Wasserstein distance. We further saw that batch Wasserstein estimators may yield false (Section 5.3) or undesirable (Section 5.4) minima.

In this section, we will show that even if some of these problems are mitigated, the resulting generators will produce undesirable images. This observation is based on the fact that the euclidean metric, i.e. the L_2 -distance based on pixelwise differences, is used explicitly in the primal formulation of the Wasserstein distance in (1.1) and implicitly in its dual formulation (1.2). We make the following conjecture: The use of the euclidean metric in the definition of the

Wasserstein distance (1.1)–(1.2) is fundamentally unsuited for image data in the context of generative models.

6.1. Mitigation of sample complexity issues

In the following, let $W_{1,\epsilon}$ be the regularized Wasserstein distance introduced by (Cuturi, 2013)

$$W_{1,\epsilon}(p^*, p^\theta) := \inf_{\gamma \in \Gamma(p^*, p^\theta)} (\mathbb{E}_{(x,y) \sim \gamma} [\|x - y\|] + \epsilon \text{KL}(\gamma \mid p^* \otimes p^\theta)),$$

where the infimum is taken over all joint distributions γ with marginals p^* and p^θ , \otimes denotes the product measure and KL is the Kullback-Leibler divergence.

Since $W_{1,\epsilon}(p, p) \neq 0$, following (Genevay et al., 2017), we use the Sinkhorn divergence $\mathcal{S}_{1,\epsilon}$ defined as

$$\mathcal{S}_{1,\epsilon}(p^*, p^\theta) = W_{1,\epsilon}(p^*, p^\theta) - \frac{1}{2} (W_{1,\epsilon}(p^*, p^*) + W_{1,\epsilon}(p^\theta, p^\theta)),$$

which is a normalized version of $W_{1,\epsilon}$ satisfying $\mathcal{S}_{1,\epsilon}(p, p) = 0$.

For $\epsilon \rightarrow 0$, $\mathcal{S}_{1,\epsilon}$ converges to the Wasserstein distance, whereas for $\epsilon \rightarrow \infty$, it converges to the maximum mean discrepancy (MMD) (Feydy et al., 2018). Since the MMD is insensitive to the curse of dimensionality (Genevay et al., 2019), the Sinkhorn divergence can be viewed as an approximation of the Wasserstein distance, which does not suffer from sample complexity issues. In particular, asymptotically as $\epsilon \rightarrow \infty$, we have

$$\mathbb{E}[\|\mathcal{S}_{1,\epsilon}(p_n^*, p_n^\theta) - \mathcal{S}_{1,\epsilon}(p^*, p^\theta)\|] = O\left(\frac{1}{\sqrt{n}}\right),$$

where p_n^*, p_n^θ are batches of size n from p^*, p^θ , respectively.

To visualize the effect on regularisation on sample complexity, we repeat the experiments from Section 5.2. The setup is exactly the same as before, except we use Sinkhorn divergence with regularisation parameter $\epsilon = 100$ instead of the Wasserstein distance. We compute the Sinkhorn divergence between the sample batches using the Sinkhorn iterations (Cuturi, 2013). The results are visualized in Figure 13. We can see that for sample size $n = 500$ the value of expected Sinkhorn divergence is already close to 0 (contrary to what we have seen with Wasserstein distance in Section 5.2).

In (Mallasto et al., 2019b), a method for the estimation of batch Sinkhorn distances during GAN training was introduced, which is called the (c, ϵ) -transform. Surprisingly, even for high values of ϵ and thus despite a better sample complexity, the generative performance remains poor (as already noticed by (Mallasto et al., 2019b)). The generator

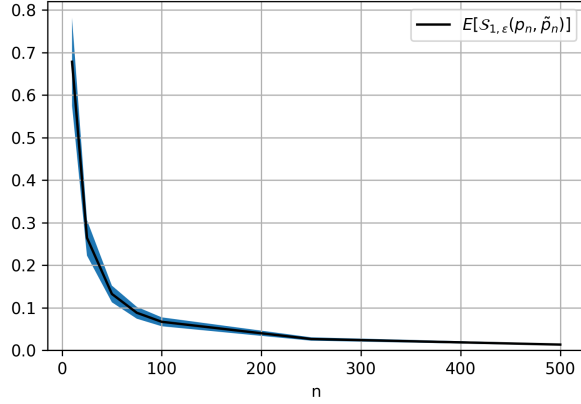


Figure 13: For high values of ϵ (here $\epsilon = 100$), the Sinkhorn divergence has a much better sample complexity than Wasserstein distance. Here the same experiment as in Figure 8 was conducted. We can see that for sample size 500 the value of sample Sinkhorn divergence is already close to 0 (contrary to batch Wasserstein distance).

converges to a geometric k -medians-like distribution. The outputs, obtained in the same way as in Section 4.2, except that we replace the c -transform by the (c, ϵ) -transform, are visualised in Figure 14. This demonstrates that mitigating sample complexity issues does not solve the problems with WGANs.

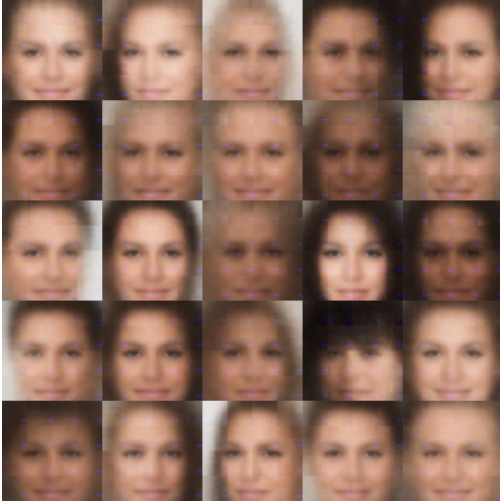


Figure 14: The output of WGAN trained using (c, ϵ) -transform with $\epsilon = 1000$.

6.2. Mitigation of discriminator suboptimality issues

If we want to use the batch Wasserstein distance or Sinkhorn divergence as a loss for a generative model, we may take ad-

vantage of the fact that computation of Sinkhorn divergence admits automatic differentiation (Genevay et al., 2017). Therefore we may replace the learnable discriminator by the true batch Sinkhorn distance and still compute the gradients using backpropagation. Moreover for small values of the regularization parameter ϵ this will provide a faithful approximation of the Wasserstein distance (Feydy et al., 2018). Such framework has been examined in (Fatras et al., 2020). The authors suggest to minimise

$$\mathbb{E}_{\substack{p_n^* \sim P_n^* \\ p_n^\theta \sim P_n^\theta}} [\mathcal{S}_{1,\epsilon}(p_n^*, p_n^\theta)]$$

wrt. θ , where the expectation is estimated using mini-batches sampled from P_n^* and P_n^θ .

We emphasise that $\mathcal{S}_{1,\epsilon}$ is computed exactly for each mini-batch using the Sinkhorn algorithm (Cuturi, 2013) instead of considering the approximation of the Sinkhorn distance in the discriminator loop as in the (c, ϵ) -transform WGAN.

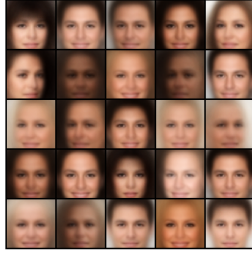
We notice that this algorithm is equivalent to training a WGAN, where the discriminator optimisation step, i.e. the inner loop in Algorithm 1, is replaced by the true batch Sinkhorn distance. For sufficiently low values of ϵ we obtain a very good approximation of the optimal discriminator dynamics of batch Wasserstein GANs where the discriminator is trained to optimality for each generator update.

The authors in (Fatras et al., 2020) showed that the algorithm is successful in learning 2D euclidean data (8-mode Gaussian mixture), but they did not perform any experiments with image data. Motivated by the failure of batch Wasserstein based losses and the connection to geometric k -medians described in the previous sections, we trained their model on image data. The result of the generator for CelebA is shown in Figure 15. Like for the c -transform, the (c, ϵ) -transform and geometric k -medians clustering which all result in low batch Wasserstein distances, we obtain non-diverse, blurry images. This demonstrates that mitigating discriminator suboptimality issues does not solve the problems with WGANs.

6.3. Fundamental failures of the L_2 -distance as a perceptual distance

Why does a Wasserstein-like distance not produce satisfactory images, even if issues related to sample complexity and suboptimality of the discriminator are mitigated? Our hypothesis is that this is due to the fact that the Wasserstein distance (and the Sinkhorn divergence) between batches of images is based on the L_2 -pixelwise distance between images. Similar conjecture has been made in (Chen et al., 2019). This can be seen from the primal formulation (1.1) of W_1 (in contrast to the dual Kantorovich-Rubinstein formulation (1.2)).

For finite point clouds p, q , we can represent them repre-


 (a) $\varepsilon = 0.01$

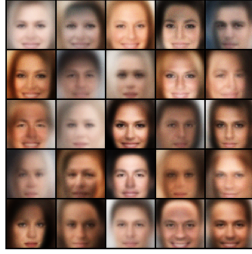
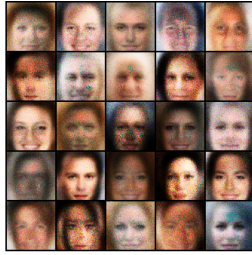
 (b) $\varepsilon = 1$

 (c) $\varepsilon = 10$

 (d) $\varepsilon = 100$

Figure 15: Images generated by a generator, which was trained using optimal discriminator dynamics, i.e. where the inner loop in Algorithm 1 is replaced by the true batch Sinkhorn distance, using the method described in (FAtlas et al., 2020). The problem of blurry, non-diverse images persists.

sented as a list of points and a list of probabilities for each point and allows to write (1.1) as

$$W_1(p, q) = \min_{\gamma \in \mathbb{R}^{m \times n}} \sum_{i,j} \gamma_{i,j} \|x_i - y_j\|_2$$

$$\text{s.t. } \gamma \mathbb{1} = P, \quad \gamma^T \mathbb{1} = Q$$

by (Peyré & Cuturi, 2020). Here, $\gamma_{i,j}$ denote the entries of the matrix $\gamma \in \mathbb{R}^{m \times n}$, x_i is the i -th image in p and y_j is j -th image in q . $P \in \mathbb{R}^n$ is such that P_i is the probability mass at x_i and $Q \in \mathbb{R}^m$ is such that Q_i is the probability mass at y_i .

When p and q both have supports of size n , the Wasserstein distance satisfies

$$W_1(p, q) = \min_{\sigma} \sum_i \|x_i - y_{\sigma(i)}\|_2,$$

where the minimisation is considered over all permutations $\sigma: \{1, \dots, n\} \rightarrow \{1, \dots, n\}$.

When optimising the batch Wasserstein distance in the context of WGANs, we consider batches p_n^*, p_n^θ of size n , drawn from the target and generated probability densities p^*, p^θ , respectively. Then, the Wasserstein distance between two batches p_n^* and p_n^θ is the sum of pixel-wise L_2 -distances, after the images in one of the batches are permuted.

In terms of the L_2 -distance, two images tend to be similar to one another, when the brightness values of their colour channels are similar. This does not necessarily meet our human perception of two images being similar. For example, while the same person photographed under different lighting conditions would be assigned a low distance by a perceptual ‘human metric’, pixelwise metrics would consider them dissimilar (which is also a reason for the specific centroids found in geometric k -medians clustering, cf. Figure 10). Wasserstein metrics on a space of distributions which are computed using pixelwise metrics on the respective sample space thus always exhibit this phenomenon. Examples of failures of the euclidean metric to capture perceptual and semantic distances between images are shown in Figure 16. We gather absurd examples, which have a lower euclidean distance to some reference image than an image, which a human would consider only a slight variation of the reference image.

Moreover, since the Wasserstein distance and the Sinkhorn divergence are metrics based on pixelwise comparisons they disregard inductive bias encoded in convolutional neural networks, which captures spatial structure present in the image data. This inductive bias is essential for the success of deep learning models (Mitchell, 2017), (Cohen & Shashua, 2017), (Ulyanov et al., 2020). In fact, in our experiments we observed that methods based on accurate approximation of the batch Wasserstein distance perform similarly regardless of training with fully-connected or convolutional architectures.

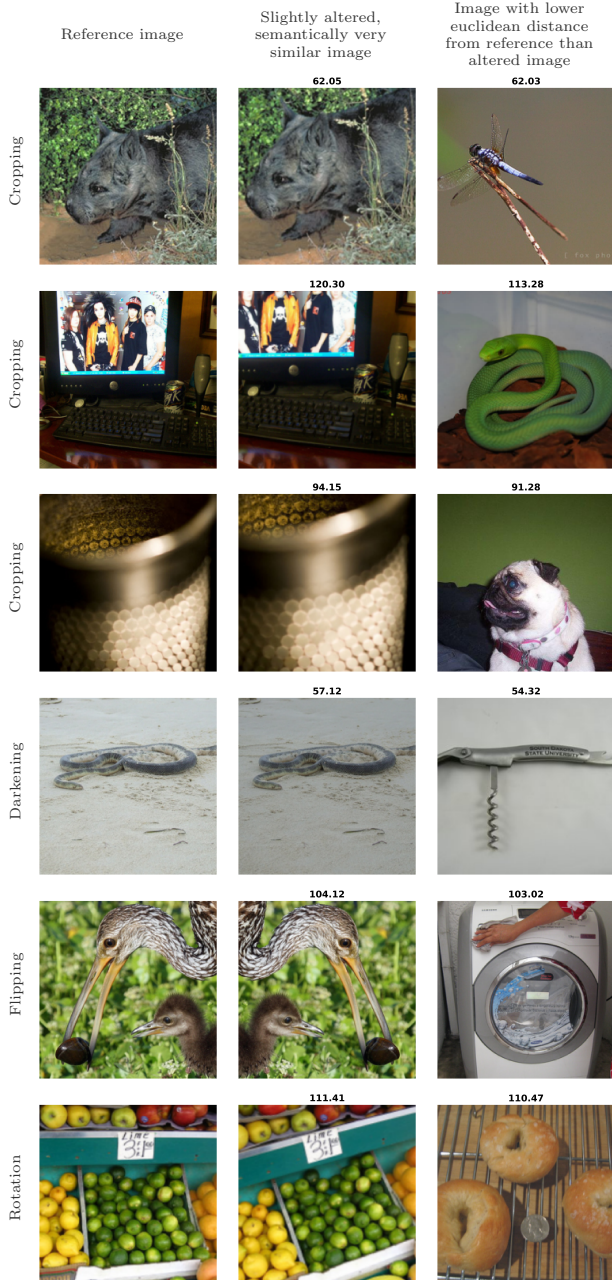


Figure 16: Examples where the L_2 -distance is not a (semantically) meaningful distance between images. In the left column, a reference image from ImageNet (Russakovsky et al., 2015) is shown. In the middle column, a slight alteration is applied, whose result a human observer would consider to be very close to the reference image. In the right column, another image from the ImageNet data set is displayed, which to the human observer is very different from the reference image, but which has a lower L_2 -distance to the reference image than the altered image. The numbers above the images indicate the L_2 -distance to the reference image.

A possible explanation why WGAN-GP (and in fact other GANs) produce high-fidelity samples is precisely because they do not approximate any statistical divergence which is based on pixelwise metrics. Contrary to those, the training dynamics lead to a discriminator which captures the similarity and dissimilarity between samples better, since they are more flexible than the simple model of pixelwise distances.

7. WGAN-GP in the space of GANs

In the previous sections, we established that the loss function of WGAN-GP does not approximate the Wasserstein distance in any meaningful sense. Moreover, accurate approximations of the Wasserstein distance are not even desirable in minibatch-based training in the typical high-dimensional setup. This leads to a natural question: *Why does WGAN-GP achieve such a good performance?* There are two possible answers in the literature which will be discussed in the following.

7.1. Lipschitz regularisation

It was suggested in (Kodali et al., 2017) and (Fedus et al., 2017) that controlling the Lipschitz constant of the discriminator may improve GAN training regardless of the statistical distance used, and that the improved performance observed in WGAN-GP was simply due to the gradient penalty term and not connected to the Wasserstein distance.

Using the architectures described in (Anil et al., 2018), we trained a WGAN and a vanilla GAN (Goodfellow et al., 2014) with a multi-layer perceptron discriminator which is provably a 1-Lipschitz function. We compared this with vanilla GAN and WGAN-GP with an ordinary unconstrained multi-layer perceptron (MLP). In both cases, we observe an improved performance when using Lipschitz constrained discriminator, even though 1-Lipschitz functions have no theoretical connection to estimating the JS-divergence (which is implicitly used in the vanilla GAN). The results on a low-dimensional learning task are visualized in Figures 17 and 18.

The importance of regularising the discriminator regardless of statistical distance used is further supported by (Schäfer et al., 2020), where authors argue that if one does not impose regularity on the discriminator, it can achieve the maximal generator loss by exploiting visually imperceptible errors in the generated images.

7.2. Does the loss function even matter?

A large-scale study (Lucic et al., 2017) in which different GAN loss functions were compared showed that GANs are very sensitive to their hyperparameter setup, and that no single loss function consistently outperforms the others. In particular it was shown that given the right hyperparam-

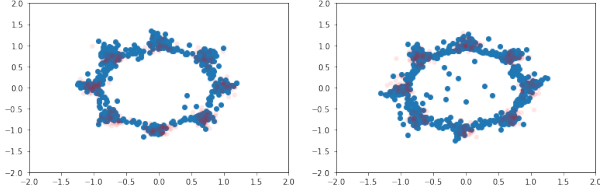


Figure 17: Two WGANs trying to learn an 8 mode Gaussian mixture. Red dots are sampled from the target distribution and blue dots are sampled from the trained generator. Left: WGAN with gradient penalty. Right: WGAN with Lipschitz discriminator.

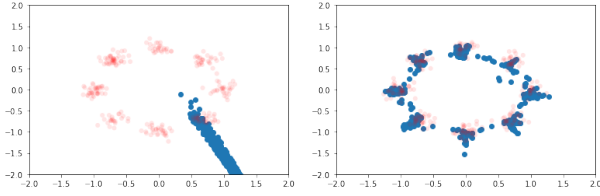


Figure 18: Left: Non saturating GAN with MLP discriminator. Right: Non saturating GAN with Lipschitz discriminator. Both trained using the same hyperparameters and computation time.

ter configuration, vanilla GAN (referred to as NS GAN in this study) can achieve a comparable or better performance than WGAN-GP. The study examined many different flavors of GANs (MM GAN (Goodfellow et al., 2014), NS GAN (Goodfellow et al., 2014), DRAGAN (Kodali et al., 2017), WGAN (Arjovsky et al., 2017), WGAN GP (Gulrajani et al., 2017), LS GAN (Mao et al., 2017), BEGAN (Berthelot et al., 2017)) on 4 benchmark data sets (MNIST, Fashion-MNIST, CIFAR10, CelebA). Each type of GAN had a different loss function and was trained with 100 different hyperparameter configurations. The hyperparameter configurations were randomly selected from a wide range of possible values. The results of the study show that given the right hyperparameter configuration, vanilla GAN can achieve a performance very close to WGAN-GP. Therefore, the initially reported success of WGAN may be a result of a lucky hyperparameter configuration and the precise loss function may be less relevant.

8. Conclusions

In this article, we examine several ways in which the theoretical foundations and the practical implementation of WGANs fundamentally differ. We argue that for good WGANs, the loss function typically does not approximate the Wasserstein distance well. Additionally, we gather evidence that good generators do not produce high-quality images *despite* a poor approximation by the discriminator,

but precisely *because* it does not approximate the batch Wasserstein distance well.

In Section 4, we show that the WGAN-GP loss function (which yields good generators) is not a meaningful approximation of W_1 due to the poor approximation of the optimal discriminator. We point out that even if the optimal discriminator is approximated accurately via the (c, ε) -transform, the resulting loss function does not improve the performance of the model, as it exhibits problems such as ‘false’ global minima. We show that these problems are significant in practice and point towards a possible reason, why this is the case (Section 5). Moreover, as we argue in Section 6, even if we eliminate all the *practical* problems listed above, the Wasserstein distance would still not be a suitable loss function, as the Wasserstein distance is based on a pixelwise distance in sample space which does not pose a perceptual distance metric.

On the contrary, we assume that the flexibility of not approximating a statistical metric based on a pixelwise metric gives rise to better discriminator (critic) networks. We partially attribute the claimed improvement in performance of WGAN over vanilla GAN to a control over the Lipschitz constant of the discriminator (Section 7.1). Moreover, some evidence suggests that the particular choice of the loss function does not impose a significant impact on the model performance (Section 7.2). Due to the above reasons, we conclude that the (true) Wasserstein distance is not a desirable loss function for GANs, and that WGANs should not be thought of as Wasserstein distance minimisers.

In future work, we would like to understand the role of the optimisation dynamics better. This concerns the two-player game between the generator and discriminator. Moreover, we would like to explore if WGANs can be modified so that they minimise a divergence based on a perceptually meaningful metric. A successful algorithm minimising optimal transport based distances needs to simultaneously address the following issues:

- Sample complexity: Possibly by regularisation (Genevay et al., 2019) or sliced distances (Deshpande et al., 2018), (Paty & Cuturi, 2019).
- Replacing the L_2 -norm by a perceptually meaningful notion of distance: We intend to explore an optimal transport distance based on L_2 between VGG embeddings of the images in future work.
- Approximation of optimal discriminator: Possibly by changing the optimisation algorithm.

Acknowledgements

JS, LMK, CE and CBS thank Anton Mallasto for sharing the code used for his experiments. JS, LMK and CBS ac-

knowledge support from the Cantab Capital Institute for the Mathematics of Information. CE and CBS acknowledge support from the Wellcome Innovator Award RG98755. LMK and CBS acknowledge support from the European Union Horizon 2020 research and innovation programmes under the Marie Skłodowska-Curie grant agreement No. 777826 (NoMADS). JS additionally acknowledges the support from Aviva. LMK additionally acknowledges support from the Magdalene College, Cambridge (Neville Research Fellowship). CBS additionally acknowledges support from the Philip Leverhulme Prize, the Royal Society Wolfson Fellowship, the EPSRC grants EP/S026045/1 and EP/T003553/1, EP/N014588/1, EP/T017961/1 and the Alan Turing Institute.

References

- Anil, C., Lucas, J., and Grosse, R. Sorting out lipschitz function approximation, 2018. URL <https://arxiv.org/abs/1811.05381>.
- Arjovsky, M. and Bottou, L. Towards principled methods for training generative adversarial networks, 2017. URL <https://arxiv.org/abs/1701.04862>.
- Arjovsky, M., Chintala, S., and Bottou, L. Wasserstein gan, 2017. URL <https://arxiv.org/abs/1701.07875>.
- Bellemare, M. G., Danihelka, I., Dabney, W., Mohamed, S., Lakshminarayanan, B., Hoyer, S., and Munos, R. The cramer distance as a solution to biased wasserstein gradients, 2017.
- Berthelot, D., Schumm, T., and Metz, L. Began: Boundary equilibrium generative adversarial networks, 2017.
- Biewald, L. Experiment tracking with weights and biases, 2020. URL <https://www.wandb.com/>. Software available from wandb.com.
- Canas, G. D. and Rosasco, L. Learning probability measures with respect to optimal transport metrics, 2012.
- Chen, Y., Telgarsky, M., Zhang, C., Bailey, B., Hsu, D., and Peng, J. A gradual, semi-discrete approach to generative network training via explicit wasserstein minimization, 2019.
- Cho, J. and Suh, C. Wasserstein gan can perform pca. In *2019 57th Annual Allerton Conference on Communication, Control, and Computing (Allerton)*, pp. 895–901, 2019. doi: 10.1109/ALLERTON.2019.8919827.
- Cohen, N. and Shashua, A. Inductive bias of deep convolutional networks through pooling geometry, 2017.
- Cuturi, M. Sinkhorn distances: Lightspeed computation of optimal transportation distances, 2013.
- Deshpande, I., Zhang, Z., and Schwing, A. Generative modeling using the sliced wasserstein distance, 2018. URL <https://arxiv.org/abs/1803.11188>.
- Erdmann, M., Geiger, L., Glombitza, J., and Schmidt, D. Generating and refining particle detector simulations using the wasserstein distance in adversarial networks, 2018.
- Fatras, K., Zine, Y., Flamary, R., Gribonval, R., and Courty, N. Learning with minibatch wasserstein : asymptotic and gradient properties, 2020.
- Fedus, W., Rosca, M., Lakshminarayanan, B., Dai, A. M., Mohamed, S., and Goodfellow, I. Many paths to equilibrium: Gans do not need to decrease a divergence at every step, 2017. URL <https://arxiv.org/abs/1710.08446>.
- Feydy, J., S  journ  , T., Vialard, F.-X., Amari, S.-I., Trouv  , A., and Peyr  , G. Interpolating between optimal transport and mmd using sinkhorn divergences, 2018.
- Flamary, R., Courty, N., Gramfort, A., Alaya, M. Z., Boissunon, A., Chambon, S., Chapel, L., Corenflos, A., Fatras, K., Fournier, N., Gautheron, L., Gayraud, N. T., Janati, H., Rakotomamonjy, A., Redko, I., Rolet, A., Schutz, A., Seguy, V., Sutherland, D. J., Tavenard, R., Tong, A., and Vayer, T. Pot: Python optimal transport. *Journal of Machine Learning Research*, 22(78):1–8, 2021. URL <http://jmlr.org/papers/v22/20-451.html>.
- Genevay, A., Peyr  , G., and Cuturi, M. Learning generative models with sinkhorn divergences, 2017. URL <https://arxiv.org/abs/1706.00292>.
- Genevay, A., Chizat, L., Bach, F., Cuturi, M., and Peyr  , G. Sample complexity of sinkhorn divergences, 2019.
- Goodfellow, I. J., Pouget-Abadie, J., Mirza, M., Xu, B., Warde-Farley, D., Ozair, S., Courville, A., and Bengio, Y. Generative adversarial networks, 2014. URL <https://arxiv.org/abs/1406.2661>.
- Graf, S., Luschgy, H., and Pag  s, G. Distortion mismatch in the quantization of probability measures. *ESAIM: Probability and Statistics*, 12:127–153, 2008. doi: 10.1051/ps:2007044.
- Gulrajani, I., Ahmed, F., Arjovsky, M., Dumoulin, V., and Courville, A. Improved training of wasserstein gans, 2017. URL <https://arxiv.org/abs/1704.00028>.

- Huang, Z., Wu, J., and Gool, L. V. Manifold-valued image generation with wasserstein generative adversarial nets, 2019.
- Karras, T., Laine, S., and Aila, T. A style-based generator architecture for generative adversarial networks, 2018. URL <https://arxiv.org/abs/1812.04948>.
- Kodali, N., Abernethy, J., Hays, J., and Kira, Z. On convergence and stability of gans, 2017. URL <https://arxiv.org/abs/1705.07215>.
- Krizhevsky, A. Learning multiple layers of features from tiny images. Technical report, University of Toronto, 2009. URL <http://www.cs.toronto.edu/~kriz/cifar.html>.
- Le, T.-N., Habrard, A., and Sebban, M. Deep multi-wasserstein unsupervised domain adaptation. *Pattern Recognition Letters*, 125:249–255, 2019a. ISSN 0167-8655. doi: <https://doi.org/10.1016/j.patrec.2019.04.025>. URL <https://www.sciencedirect.com/science/article/pii/S0167865519301400>.
- Le, T.-N., Habrard, A., and Sebban, M. Deep multi-wasserstein unsupervised domain adaptation. *Pattern Recognition Letters*, 125:249–255, 2019b. ISSN 0167-8655. doi: <https://doi.org/10.1016/j.patrec.2019.04.025>. URL <https://www.sciencedirect.com/science/article/pii/S0167865519301400>.
- Lei, N., Su, K., Cui, L., Yau, S.-T., and Gu, X. D. A geometric view of optimal transportation and generative model. *Computer Aided Geometric Design*, 68:1–21, 2019. ISSN 0167-8396. doi: <https://doi.org/10.1016/j.cagd.2018.10.005>. URL <https://www.sciencedirect.com/science/article/pii/S0167839618301249>.
- Liu, Z., Luo, P., Wang, X., and Tang, X. Deep learning face attributes in the wild. In *Proceedings of International Conference on Computer Vision (ICCV)*, December 2015.
- Lloyd, S. Least squares quantization in pcm. *IEEE transactions on information theory*, 28(2):129–137, 1982.
- Lucic, M., Kurach, K., Michalski, M., Gelly, S., and Bousquet, O. Are gans created equal? a large-scale study, 2017. URL <https://arxiv.org/abs/1711.10337>.
- Lunz, S., Öktem, O., and Schönlieb, C.-B. Adversarial regularizers in inverse problems, 2019.
- Mallasto, A., Frellsen, J., Boomsma, W., and Feragen, A. (q,p)-wasserstein gans: Comparing ground metrics for wasserstein gans, 2019a. URL <https://arxiv.org/abs/1902.03642>.
- Mallasto, A., Montúfar, G., and Gerolin, A. How well do wgans estimate the wasserstein metric?, 2019b.
- Mao, X., Li, Q., Xie, H., Lau, R. Y. K., Wang, Z., and Smolley, S. P. Least squares generative adversarial networks, 2017.
- Mitchell, B. The spatial inductive bias of deep learning, 2017. URL <http://jhir.library.jhu.edu/handle/1774.2/40864>.
- Miyato, T., Kataoka, T., Koyama, M., and Yoshida, Y. Spectral normalization for generative adversarial networks, 2018. URL <https://arxiv.org/abs/1802.05957>.
- Narayanan, H. and Mitter, S. Sample complexity of testing the manifold hypothesis. In *Proceedings of the 23rd International Conference on Neural Information Processing Systems - Volume 2, NIPS’10*, pp. 1786–1794, Red Hook, NY, USA, 2010. Curran Associates Inc.
- Paty, F.-P. and Cuturi, M. Subspace robust wasserstein distances, 2019.
- Pedregosa, F., Varoquaux, G., Gramfort, A., Michel, V., Thirion, B., Grisel, O., Blondel, M., Prettenhofer, P., Weiss, R., Dubourg, V., et al. Scikit-learn: Machine learning in python. *the Journal of machine Learning research*, 12:2825–2830, 2011.
- Peyré, G. and Cuturi, M. Computational optimal transport, 2020.
- Pinetz, T., Soukup, D., and Pock, T. On the estimation of the wasserstein distance in generative models, 2019.
- Pope, P., Zhu, C., Abdelkader, A., Goldblum, M., and Goldstein, T. The intrinsic dimension of images and its impact on learning, 2021.
- Radford, A., Metz, L., and Chintala, S. Unsupervised representation learning with deep convolutional generative adversarial networks, 2016.
- Russakovsky, O., Deng, J., Su, H., Krause, J., Satheesh, S., Ma, S., Huang, Z., Karpathy, A., Khosla, A., Bernstein, M., et al. Imagenet large scale visual recognition challenge. *International journal of computer vision*, 115(3): 211–252, 2015.
- Schäfer, F., Zheng, H., and Anandkumar, A. Implicit competitive regularization in gans, 2020.
- Ulyanov, D., Vedaldi, A., and Lempitsky, V. Deep image prior. *International Journal of Computer Vision*, 128(7): 1867–1888, Mar 2020. ISSN 1573-1405. doi: [10.1007/s11263-020-01303-4](https://doi.org/10.1007/s11263-020-01303-4). URL <http://dx.doi.org/10.1007/s11263-020-01303-4>.

Weed, J. and Bach, F. Sharp asymptotic and finite-sample rates of convergence of empirical measures in wasserstein distance, 2017.

Weiszfeld, E. Sur le point pour lequel la somme des distances de n points donnés est minimum. *Tohoku Mathematical Journal, First Series*, 43:355–386, 1937.

Weng, L. From gan to wgan, 2019.

A. Geometric k-medians

A.1. Formal definitions and proofs

Following (Graf et al., 2008), we define the nearest neighbour projection:

Definition A.1.1 (Nearest neighbour projection). Let $S \subseteq \mathbb{R}^d$ be a closed set. A nearest neighbour projection on S is denoted by π_S and defined as

$$\pi_S(x) = \sum_{s \in S} s 1_{B_s(S)}(x), \quad x \in \mathbb{R}^d,$$

where $1_{B_s(S)}$ is the indicator function of $B_s(S)$ and $B(S) := (B_s(S))_{s \in S}$ is a Borel Voronoi partition of \mathbb{R}^d such that $B_s(S) \subseteq \{x \in \mathbb{R}^d : \|x - s\| = \min_{\tilde{s} \in S} \|x - \tilde{s}\|\}$.

Interested readers are referred to (Graf et al., 2008) for technical details.

Remark 4. If S is a finite set, then π_S maps x to a point in S with minimal distance from x . If S is not convex this point may be dependent on the choice of the Voronoi partition $B(S)$.

Definition A.1.2 (Projection measure). Let $S \subseteq \mathbb{R}^d$ be a closed set and let π_S be a nearest neighbour projection on S . Moreover, let ρ be a probability distribution on \mathbb{R}^d . Then $\pi_S \rho$ denotes the distribution obtained as a push-forward of ρ by π_S , i.e. $\pi_S \rho(A) = \rho(\pi_S^{-1}(A))$ for any $A \subset \mathbb{R}^d$.

Lemma A.1.1 ((Canas & Rosasco, 2012)). Fix $1 \leq p < \infty$. Let $S \subseteq \mathbb{R}^d$ be a closed set, and let ρ be a probability distribution on \mathbb{R}^d with finite p-th moment. We have

$$\mathbb{E}_{x \sim \rho} d(x, S)^p = W_p(\rho, \pi_S \rho)^p,$$

where $d(x, S)$ denotes the distance the smallest distance from x to S and W_p is the Wasserstein-p metric.

Lemma A.1.2 ((Canas & Rosasco, 2012)). Fix $1 \leq p < \infty$. Let $S \subseteq \mathbb{R}^d$ be a closed set, and let ρ be a probability distribution on \mathbb{R}^d with finite p-th moment. For all probability distributions μ with finite p-th moment such that $\text{supp}(\mu) \subseteq S$, we have

$$W_p(\rho, \mu) \geq W_p(\rho, \pi_S \rho).$$

Definition A.1.3 (Geometric k medians). Let $\mathcal{X} = \{x_i, i = 1, \dots, n\}$ be a data set in \mathbb{R}^d . Given an arbitrary set $S = \{m_i, i = 1, \dots, k\} \subseteq \mathbb{R}^d$, let $S_i = \{x \in \mathcal{X} : m_i = \arg \min_{m \in S} \|m - x\|_2\}$, i.e. S_i consists of the points in \mathcal{X} for which the closest point in S is m_i . The *geometric k -medians* is defined as the set $\hat{S} = \{\hat{m}_i, i = 1, \dots, k\}$ such that

$$\begin{aligned} \hat{S} &:= \arg \min_{S \subseteq \mathbb{R}^d : |S|=k} \sum_{i=1}^k \sum_{x \in S_i} d(x, m_i) \\ &= \arg \min_{S \subseteq \mathbb{R}^d : |S|=k} \sum_{x \in \mathcal{X}} d(x, S). \end{aligned}$$

Theorem A.1.3. Let $\mathcal{X} = \{x_i, i = 1, \dots, n\}$ be a data set in \mathbb{R}^d and let $\rho := \frac{1}{n} \sum_{i=1}^n \delta_{x_i}$ be the associated empirical measure. Moreover, let $\hat{S} = \{\hat{m}_i, i = 1, \dots, k\}$ be the geometric k -medians for \mathcal{X} and let $\hat{S}_i := \{x \in \mathcal{X} : \hat{m}_i = \arg \min_{m \in \hat{S}} \|m - x\|_2\}$, i.e. the points in \mathcal{X} for which the closest point in \hat{S} is \hat{m}_i . Then,

$$\pi_{\hat{S}} \rho = \arg \min_{\mu : \text{supp}(\mu)=k} W_1(\rho, \mu),$$

where $\pi_{\hat{S}} = \frac{1}{n} \sum_{i=1}^n \delta_{\pi_{\hat{S}}(x_i)} = \sum_{i=1}^k \frac{|\hat{S}_i|}{n} \delta_{\hat{m}_i}$.

Since $\pi_{\hat{S}} \rho$ is an empirical measure concentrated on \hat{S} , Theorem A.1.3 states that the empirical distribution concentrated on geometric k -medians is the minimiser of the Wasserstein-1 distance between the empirical distribution of the data \mathcal{X} and all distributions μ with $\text{supp}(\mu) = k$.

Proof. We can proceed in close analogy with (Canas & Rosasco, 2012) where a connection between k -means and W_2 is examined. We have

$$\begin{aligned} \hat{S} &= \arg \min_{S \subseteq \mathbb{R}^d : |S|=k} \sum_{x \in \mathcal{X}} d(x, S) = \arg \min_{S \subseteq \mathbb{R}^d : |S|=k} \frac{1}{n} \sum_{x \in \mathcal{X}} d(x, S) \\ &= \arg \min_{S \subseteq \mathbb{R}^d : |S|=k} \mathbb{E}_{x \sim \rho} d(x, S) = \arg \min_{S \subseteq \mathbb{R}^d : |S|=k} W_1(\rho, \pi_S \rho), \end{aligned}$$

where the last equality follows from Lemma A.1.1. Hence,

$$\pi_{\hat{S}} \rho = \arg \min_{\pi_S \rho : S \subseteq \mathbb{R}^d, |S|=k} W_1(\rho, \pi_S \rho).$$

This means that $\pi_{\hat{S}} \rho$ minimises the Wasserstein distance from ρ among all measures which are projections on a set S supported on k points. On the other hand, we know that a projection measure always minimises the Wasserstein over all measures with support contained in a set S (Lemma A.1.2). Together, this implies that $\pi_{\hat{S}} \rho$ minimises Wasserstein distance among all measures with support contained in a set S supported on k points. \square

B. Differences to previous experiments

Here we explain crucial differences between three seemingly similar experiments, which explore different aspects of the approximation of the Wasserstein distance in WGANs. We compare our experiment described in Algorithm 4 with an experiment of Pinetz et al. (2019) described in Algorithm 5 and an experiment of Mallasto et al. (2019b) described in Algorithm 6.

Algorithm 4: Approximation Stanczuk et al

```

for  $N$  iterations do
    Sample a batch  $p_n^*$  from  $p^*$ 
    Sample a batch  $p_n^\theta$  from  $p^\theta$ 
    Ascent step on  $D_\alpha$  wrt.
         $\mathcal{V}(D_\alpha, p_n^*, p_n^\theta) - \lambda \mathcal{R}(D_\alpha, p_n^*, p_n^\theta)$ 
end
 $W_1^D(p^*, p^\theta) \leftarrow \mathbb{E}_{x \sim p^*}[D_\alpha(x)] - \mathbb{E}_{x \sim p^\theta}[D_\alpha(x)]$ 
 $W_1(p^*, p^\theta) \leftarrow$  Solution of LP for  $p^*, p^\theta$ 
Compare  $W_1^D(p^*, p^\theta)$  and  $W_1(p^*, p^\theta)$ 
    
```

Algorithm 5: Approximation Pinetz et al

```

for  $N$  iterations do
    Ascent step on  $D_\alpha$  wrt.  $\mathcal{V}(D_\alpha, p^*, p^\theta)$ 
end
 $W_1^D(p^*, p^\theta) \leftarrow \mathbb{E}_{x \sim p^*}[D_\alpha(x)] - \mathbb{E}_{x \sim p^\theta}[D_\alpha(x)]$ 
 $W_1(p^*, p^\theta) \leftarrow$  Solution for LP for  $p^*, p^\theta$ 
Compare  $W_1^D(p^*, p^\theta)$  and  $W_1(p^*, p^\theta)$ 
    
```

Algorithm 6: Approximation Mallasto et al

```

for  $N$  iterations do
    Sample a batch  $p_n^*$  from  $p^*$ 
    Sample a batch  $p_n^\theta$  from  $p^\theta$ 
    Ascent step on  $D_\alpha$  wrt.  $\mathcal{V}(D_\alpha, p_n^*, p_n^\theta)$ 
end
for  $M$  iterations do
    Sample a batch  $p_n^*$  from  $p^*$ 
    Sample a batch  $p_n^\theta$  from  $p^\theta$ 
     $W_1^D(p^*, p^\theta) \leftarrow \mathbb{E}_{x \sim p^*}[D_\alpha(x)] - \mathbb{E}_{x \sim p^\theta}[D_\alpha(x)]$ 
     $W_1(p_n^*, p_n^\theta) \leftarrow$  Solution for LP for  $p^*, p^\theta$ 
    Compare  $W_1^D(p_n^*, p_n^\theta)$  and  $W_1(p_n^*, p_n^\theta)$ 
end
    
```

Pinetz et al. (2019) take two small batches ($n = 500$) of CIFAR-10 images and train the discriminator using to WGAN-GP loss function as described in the Algorithm 5. Then the authors check how well $\mathcal{V}(D_\alpha, p^*, p^\theta)$ approximates $W_1(p^*, p^\theta)$, after the discriminator has been trained. We emphasise that the training is done using full batches

and not mini-batches, and that the measures p^*, p^θ consider small sample sizes (500 samples). Contrary to our experiment it does not examine the mini-batch dynamics used in WGAN-GP, where algorithm tries to approximate the distributional Wasserstein distance $W_1(p^*, p^\theta)$ based on many small batches p_n^* and p_n^θ .

In contrast we pick two large finitely supported distributions p^* and p^θ , each consists of 10K images from CIFAR-10 (Krizhevsky, 2009). Then we sample mini-batches of size $n = 64$ from p^*, p^θ and maximise $\mathcal{L}_D(\alpha)$. This is exactly the same procedure as in the WGAN-GP training in Algorithm 1 except that both measures are static (as if the generator in Algorithm 1 was frozen).

The experiment of (Mallasto et al., 2019b) checks the quality of minibatch estimator rather than the oracle estimator, i.e. how well on average $\mathcal{V}(D_\alpha, p_n^*, p_n^\theta)$ approximates $W_1(p_n^*, p_n^\theta)$ (after the discriminator has been trained) and not how well $\mathcal{V}(D_\alpha, p_n^*, p_n^\theta)$ approximates $W_1(p^*, p^\theta)$ from which the batches are drawn.